Supporting Information

Decoupling resource-coupled gene expression in living cells

Tatenda Shopera, Lian He, Tolutola Oyetunde, Yinjie J. Tang, and Tae Seok Moon

[1] Mathematical analysis to determine resource-coupling correlations in systems with three different circuit topologies – analytical solution

Table S1. Definition of parameters and variables used in this work.

Symbols	Definition	Symbols	Definition
k_1	dissociation constant of a ribosome binding to the RFP ribosome binding site	K_{AD}	dissociation constant for ExsA-ExsD interaction
k_2	dissociation constant of a ribosome binding to the GFP ribosome binding site	K_{u1}	half-maximal inducer concentration for the pLux* promoter
k_3	dissociation constant of a ribosome binding to the ExsA ribosome binding site	K_{u2}	half-maximal inducer concentration for the pTet* promoter
k_4	dissociation constant of a ribosome binding to the InvF ribosome binding site	K_{p1}	half-maximal ExsA concentration for the pexsD promoter
k_5	dissociation constant of a ribosome binding to the SicA ribosome binding site	K_{p2}	half-maximal InvF-SicA complex concentration for the psicA promoter
k_d	dissociation constant of a ribosome binding to the ExsD ribosome binding site	n_1	plasmid concentration (p15A)
κ_1	dissociation constant of the RNA polymerase binding to the promoter for RFP expression (pLux*)	n_2	plasmid concentration (ColE1)
κ_2	dissociation constant of the RNA polymerase binding to the promoter for GFP expression	n_3	plasmid concentration (pSC101)
κ_3	dissociation constant of the RNA polymerase binding to the promoter for ExsA or InvF-SicA expression (pTet*)	C_{LR}	concentration of complex formed between 3OC6 and LuxR
K_{IS}	dissociation constant for InvF-SicA interaction	C_{TR}	aTc concentration
μ_1	dissociation constant for the binding of inducer complex C_{LR} to the promoter for RFP	C_{IS}	concentration of 1:2 complex of InvF and SicA
μ_2	dissociation constant for the binding of ExsA or complex C_{IS} to the promoter for GFP	m_1	RFP mRNA
μ_3	dissociation constant for the binding of inducer C_{TR} to the TetR-bound promoter	m_2	GFP mRNA
δ_1	RFP mRNA decay rate	m_3	ExsA mRNA
δ_2	GFP mRNA decay rate	m_4	InvF mRNA
δ_3	ExsA mRNA decay rate	m_5	SicA mRNA
δ_4	InvF mRNA decay rate	m_d	ExsD mRNA
δ_5	SicA mRNA decay rate	c_1	activated promoter complex for RFP transcription
δ_d	ExsD mRNA decay rate	c_2	activated promoter complex for GFP transcription
λ_1	RFP decay rate	c_3	activated promoter complex for ExsA or InvF-SicA transcription
λ_2	GFP decay rate	d_1	mRNA-ribosome complex for RFP production
λ_3	ExsA decay rate	d_2	mRNA-ribosome complex for GFP production
λ_4	InvF decay rate	d_3	mRNA-ribosome complex for ExsA production
λ_5	SicA decay rate	d_4	mRNA-ribosome complex for InvF production
λ_d	ExsD decay rate	d_5	mRNA-ribosome complex for SicA production
π_1	RFP production rate	d_d	mRNA-ribosome complex for ExsD production
π_2	GFP production rate	a_1	fraction of ribosome-bound mRNA (RFP)
π_3	ExsA production rate	a_2	fraction of ribosome-bound mRNA (GFP)
π_4	InvF production rate	a_3	fraction of ribosome-bound mRNA (ExsA)
π_5	SicA production rate	a_4	fraction of ribosome-bound mRNA (InvF)
π_d	ExsD production rate	a_5	fraction of ribosome-bound mRNA (SicA)
γ_1	RFP transcription rate	a_d	fraction of ribosome-bound mRNA (ExsD)
γ_2	GFP transcription rate	b_1*	free pLux* promoter
γ_3	ExsA or InvF-SicA transcription rate	b_1	promoter complex of C_{LR} and b_1*
X	total RNA polymerase (RNAP) concentration	b_2*	free pexsD promoter or free psicA promoter
Y	total ribosome concentration	b_2	constitutive pCI, ExsA-pexsD complex, or C_{IS}-psciA complex
x	free RNA polymerase (RNAP) concentration	b_3*	TetR-pTet* complex
y	free ribosome concentration	b_3	pTet* promoter without TetR bound

System #1

1. Circuit 1 (Medium copy plasmid (MCP), p15A)

Transcriptional reactions: 3OC6 binds to LuxR and forms a complex C_{LR}, which binds to the free pLux* promoter (b_1^*). b_1 is the promoter complex of C_{LR} and b_1^*. The rate of transcription is represented by forward and reverse reaction rates κ_1^+ and κ_1^-, respectively. x denotes the free RNAP that binds to b_1 forming the activated complex (c_1), which results in production of mRNA (m_1) that codes for RFP. m_1 is produced at the rate of γ_1 and decays at the rate of δ_1.

Translational reactions: Translation of mRNA (m_1), upon binding with free ribosome (y), occurs at the rate of π_1. The RFP protein decays at the rate of λ_1. The mRNA-ribosome complex (d_1), whose formation kinetics is captured by forward and reverse rates k_1^+ and k_1^-, respectively, also decays at the rate of $a_1\delta_1$. Transcription and translation occurring in Circuit 1 upon induction with 3OC6 inducer are described by the following reactions.

***Transcriptional reactions*:**

$$C_{LR} + b_1^* \underset{\mu_1^-}{\overset{\mu_1^+}{\leftrightarrow}} b_1, \qquad b_1 + x \underset{\kappa_1^-}{\overset{\kappa_1^+}{\leftrightarrow}} c_1, \qquad c_1 \xrightarrow{\gamma_1} b_1 + x + m_1, \qquad m_1 \xrightarrow{\delta_1} \varnothing$$

***Translational reactions*:**

$$m_1 + y \underset{k_1^-}{\overset{k_1^+}{\leftrightarrow}} d_1 \xrightarrow{a_1\delta_1} y, \qquad d_1 \xrightarrow{\pi_1} m_1 + y + [RFP], \qquad [RFP] \xrightarrow{\lambda_1} \varnothing$$

***ODE models*:**

$$\frac{db_1}{dt} = \left(\mu_1^+ C_{LR} b_1^* - \mu_1^- b_1\right) - \left(\kappa_1^+ x b_1 - \kappa_1^- c_1\right) + \gamma_1 c_1 \tag{1}$$

$$\frac{dc_1}{dt} = \left(\kappa_1^+ x b_1 - \kappa_1^- c_1\right) - \gamma_1 c_1 \tag{2}$$

$$\frac{dm_1}{dt} = \gamma_1 c_1 - \delta_1 m_1 - \left(k_1^+ m_1 y - k_1^- d_1\right) + \pi_1 d_1 \tag{3}$$

$$\frac{dd_1}{dt} = \left(k_1^+ m_1 y - k_1^- d_1\right) - \pi_1 d_1 - a_1 \delta_1 d_1 \quad (4)$$

$$\frac{d[RFP]}{dt} = \pi_1 d_1 - \lambda_1 [RFP] \quad (5)$$

2. Circuit 2 (High copy plasmid (HCP), ColE1)

For the production of GFP in Circuit 2, the free RNAP (x) binds to the constitutive pCI promoter (b_2). All the parameters (subscript 2) have the same meaning as those in Circuit 1 above.

***Transcriptional reactions*:**

$$b_2 + x \underset{\kappa_2^-}{\overset{\kappa_2^+}{\leftrightarrow}} c_2, \quad c_2 \xrightarrow{\gamma_2} b_2 + x + m_2, \quad m_2 \xrightarrow{\delta_2} \varnothing$$

***Translational reactions*:**

$$m_2 + y \underset{k_2^-}{\overset{k_2^+}{\leftrightarrow}} d_2 \xrightarrow{a_2\delta_2} y, \quad d_2 \xrightarrow{\pi_2} m_2 + y + [GFP], \quad [GFP] \xrightarrow{\lambda_2} \varnothing$$

***ODE models*:**

$$\frac{db_2}{dt} = \gamma_2 c_2 - \left(\kappa_2^+ x b_2 - \kappa_2^- c_2\right) \quad (6)$$

$$\frac{dc_2}{dt} = \left(\kappa_2^+ x b_2 - \kappa_2^- c_2\right) - \gamma_2 c_2, \quad (7)$$

$$\frac{dm_2}{dt} = \gamma_2 c_2 - \delta_2 m_2 - \left(k_2^+ m_2 y - k_2^- d_2\right) + \pi_2 d_2, \quad (8)$$

$$\frac{dd_2}{dt} = \left(k_2^+ m_2 y - k_2^- d_2\right) - \pi_2 d_2 - a_2 \delta_2 d_2, \quad (9)$$

$$\frac{d[GFP]}{dt} = \pi_2 d_2 - \lambda_2 [GFP] \quad (10)$$

***Mass balances*:**

Since the total concentrations of DNA (n_i), RNAP (X), and ribosome (Y) are conserved, we can write the following mass balances:

$$n_1 = b_1^* + b_1 + c_1 \quad \text{(MCP, p15A)} \tag{11}$$

$$n_2 = b_2 + c_2 \quad \text{(HCP, ColE1)} \tag{12}$$

$$X = x + c_1 + c_2 \quad \text{(RNAP)} \tag{13}$$

$$Y = y + d_1 + d_2 \quad \text{(Ribosome)} \tag{14}$$

At steady state and using the assumptions and simplifications defined in Box 1, the slope of the GFP – RFP curve for System #1 is

$$\frac{-n_1\left(A_1+B_1\right)}{n_2\left(A_2X+B_2+C_2\right)} \tag{15}$$

where n_1, n_2, A_1, A_2, B_1, B_2, C_2, and X are all constants. Thus, the relationship between RFP and GFP is linear. Details of the derivation of this equation have also been described (1).

Box 1: Notations and simplifications

The following equations are used to simplify the mathematical analysis (assuming steady state) (1).

$$\kappa_i = \frac{\kappa_i^- + \gamma_i}{\kappa_i^+}, \qquad k_i = \frac{k_i^- + \pi_i + a_i\delta_i}{a_i k_i^+}, \qquad h_i = \frac{\gamma_i n_i}{a_i \delta_i}, \quad q_i = \frac{\pi_i}{\lambda_i} h_i, \quad \mu_i = \frac{\mu_i^-}{\mu_i^+}$$

$\kappa_i \gg x$ and $k_i \gg y$ (concentrations of free RNAP and ribosome are low at low growth rates).

$$A_i = \frac{\lambda_i}{\pi_i}, \quad B_i = k_i \frac{a_i \delta_i \lambda_i}{\pi_i \gamma_i}, \quad C_i = \frac{\kappa_i B_i}{n_i}$$

System #1

$$\varepsilon = \frac{\frac{C_{LR}}{\mu_1}\left(1+\frac{x}{\kappa_1}\right)}{1+\frac{C_{LR}}{\mu_1}\left(1+\frac{x}{\kappa_1}\right)}$$

System #2

$$\varepsilon_1 = \frac{\frac{C_{LR}}{\mu_1}\left(1+\frac{x}{\kappa_1}\right)}{1+\frac{C_{LR}}{\mu_1}\left(1+\frac{x}{\kappa_1}\right)}, \quad \varepsilon_2 = \frac{\frac{[ExsA]}{\mu_2}\left(1+\frac{x}{\kappa_2}\right)}{1+\frac{[ExsA]}{\mu_2}\left(1+\frac{x}{\kappa_2}\right)}, \quad \varepsilon_3 = \frac{\frac{C_{TR}}{\mu_3}\left(1+\frac{x}{\kappa_3}\right)}{1+\frac{C_{TR}}{\mu_3}\left(1+\frac{x}{\kappa_3}\right)}$$

$$K_1 = \kappa_1\kappa_3 B_1 B_3 + \varepsilon_3\left(\kappa_1 B_1 B_3 n_3 + \kappa_1 B_1 X A_3 n_3\right)$$

$$K_2 = \kappa_3 B_1 B_3 n_1 + \kappa_3 B_3 X A_1 n_1$$

$$K_3 = \kappa_2\kappa_3 B_2 B_3 + \varepsilon_3\left(\kappa_2 B_2 B_3 n_3 + \kappa_3 B_3 X A_2 n_3\right)$$

$$K_4 = \kappa_3 B_2 B_3 n_2 + \kappa_3 B_3 X A_2 n_2$$

System #3

$$\varepsilon_1 = \frac{\frac{C_{LR}}{\mu_1}\left(1+\frac{x}{\kappa_1}\right)}{1+\frac{C_{LR}}{\mu_1}\left(1+\frac{x}{\kappa_1}\right)}, \quad \varepsilon_2 = \frac{\frac{[C_{IS}]}{\mu_2}\left(1+\frac{x}{\kappa_2}\right)}{1+\frac{[C_{IS}]}{\mu_2}\left(1+\frac{x}{\kappa_2}\right)}, \quad \varepsilon_3 = \frac{\frac{C_{TR}}{\mu_3}\left(1+\frac{x}{\kappa_3}\right)}{1+\frac{C_{TR}}{\mu_3}\left(1+\frac{x}{\kappa_3}\right)}$$

$$K_5 = \kappa_1\kappa_3 B_1 B_4 B_5 + \varepsilon_3(\kappa_1 B_1 B_4 B_5 n_3 + \kappa_1 B_1 B_5 X A_4 n_3 + \kappa_3 B_1 B_4 X A_5 n_3)$$

$$K_6 = \kappa_3 B_1 B_4 B_5 n_1 + \kappa_3 B_4 B_5 X A_1 n_1$$

$$K_7 = \kappa_2\kappa_3 B_2 B_4 B_5 + \varepsilon_3(\kappa_2 B_2 B_4 B_5 n_3 + \kappa_3 B_4 B_5 X A_2 n_3 + \kappa_3 B_1 B_4 X A_5 n_3)$$

$$K_8 = \kappa_3 B_2 B_4 B_5 n_2 + \kappa_3 B_4 B_5 X A_2 n_2$$

System #2

1. Circuit 1 is identical to that of System #1.

2. Circuit 2

In this circuit, aTc (C_{TR}) is the inducer for the pTet* promoter controlling the expression of the transcription factor ExsA. C_{TR} activates the pTet* promoter (b_3) by binding the TetR repressor that is initially in the TetR-

pTet* complex (b_3^*). $[ExsA]_0$ and [ExsA] represent the total and the free ExsA concentration in the system, respectively. Here, transcription and translation parameters for ExsA are shown with subscript 3 while those of GFP are with 2. ExsA is the activator for GFP expression. All parameters have the same meaning as defined earlier.

***Trascriptional reactions*:**

$$C_{TR} + b_3^* \underset{\mu_3^-}{\overset{\mu_3^+}{\leftrightarrow}} b_3, \qquad b_3 + x \underset{\kappa_3^-}{\overset{\kappa_3^+}{\leftrightarrow}} c_3, \qquad c_3 \xrightarrow{\gamma_3} b_3 + x + m_3, \qquad m_3 \xrightarrow{\delta_3} \varnothing$$

$$[ExsA] + b_2^* \underset{\mu_2^-}{\overset{\mu_2^+}{\leftrightarrow}} b_2, \qquad b_2 + x \underset{\kappa_2^-}{\overset{\kappa_2^+}{\leftrightarrow}} c_2, \qquad c_2 \xrightarrow{\gamma_2} b_2 + x + m_2, \qquad m_2 \xrightarrow{\delta_2} \varnothing$$

***Translational reactions*:**

$$m_3 + y \underset{k_3^-}{\overset{k_3^+}{\leftrightarrow}} d_3 \xrightarrow{a_3\delta_3} y, \qquad d_3 \xrightarrow{\pi_3} m_3 + y + [ExsA]_0, \qquad [ExsA]_0 \xrightarrow{\lambda_3} \varnothing$$

$$m_2 + y \underset{k_2^-}{\overset{k_2^+}{\leftrightarrow}} d_2 \xrightarrow{a_2\delta_2} y, \qquad d_2 \xrightarrow{\pi_2} m_2 + y + [GFP], \qquad [GFP] \xrightarrow{\lambda_2} \varnothing$$

***ODE models*:**

$$\frac{db_2}{dt} = \left(\mu_2^+ [ExsA] b_2^* - \mu_2^- b_2\right) - \left(\kappa_2^+ x b_2 - \kappa_2^- c_2\right) + \gamma_2 c_2, \tag{16}$$

$$\frac{db_3}{dt} = \left(\mu_3^+ C_{TR} b_3^* - \mu_3^- b_3\right) - \left(\kappa_3^+ x b_3 - \kappa_3^- c_3\right) + \gamma_3 c_3, \tag{17}$$

$$\frac{dc_i}{dt} = \left(\kappa_i^+ x b_i - \kappa_i^- c_i\right) - \gamma_i c_i, \qquad i \in \{2,3\} \tag{18-19}$$

$$\frac{dm_i}{dt} = \gamma_i c_i - \delta_i m_i - (k_i^+ m_i y - k_i^- d_i) + \pi_i d_i, \quad i \in \{2,3\} \tag{20-21}$$

$$\frac{dd_i}{dt} = \left(k_i^+ m_i y - k_i^- d_i\right) - \pi_i d_i - a_i \delta_i d_i, \; i \in \{2,3\} \tag{22-23}$$

$$\frac{d[\text{ExsA}]_0}{dt} = \pi_3 d_3 - \lambda_3 [\text{ExsA}]_0 . \quad (24)$$

$$\frac{d[\text{GFP}]}{dt} = \pi_2 d_2 - \lambda_2 [\text{GFP}]. \quad (25)$$

***Mass balances*:**

We can write similar mass balances as in System #1 for the different plasmids, RNAP, and ribosome. In addition, we have a mass balance equation for ExsA, where $[\text{ExsA}]_0$ and [ExsA] are the total and free concentration of ExsA, respectively.

$n_i = b_i^* + b_i + c_i$, $i \in \{1,2,3\}$ (Plasmids 1, 2, and 3 are p15A, ColE1, and pSC101, respectively) (26-28)

$$X = x + \sum_{i=1}^{3} c_i \quad (29)$$

$$Y = y + \sum_{i=1}^{3} d_i \quad (30)$$

$$[\text{ExsA}]_0 = [\text{ExsA}] + b_2 \quad (31)$$

The steady state relationship between GFP and RFP for System #2 is derived as follows:

Change in inducer concentration [3OC6] causes change in system variables. The change in [GFP] with respect to that of [RFP] can be shown to be

$$\frac{\Delta[\text{GFP}]}{\Delta[\text{RFP}]} = \frac{(\kappa_1\kappa_3 B_1 B_3)(\varepsilon_2'-\varepsilon_2)+(\kappa_3 B_1 B_3 n_1+\kappa_3 B_3 X A_1 n_1)(\varepsilon_1\varepsilon_2'-\varepsilon_1'\varepsilon_2)+(\kappa_1 B_1 B_3 n_3+\kappa_1 B_1 X A_3 n_3)(\varepsilon_2'\varepsilon_3-\varepsilon_2\varepsilon_3')}{(\kappa_2\kappa_3 B_2 B_3)(\varepsilon_1'-\varepsilon_1)-(\kappa_3 B_2 B_3 n_2+\kappa_3 B_3 X A_2 n_2)(\varepsilon_1\varepsilon_2'-\varepsilon_1'\varepsilon_2)+(\kappa_2 B_2 B_3 n_3+\kappa_3 B_3 X A_2 n_3)(\varepsilon_1'\varepsilon_3-\varepsilon_1\varepsilon_3')}$$

where the prime denotes the new values of the variables due to the change in 3OC6. From the assumptions in Box 1, the change in ε_3 can be neglected, that is $\varepsilon_3 = \varepsilon_3'$. Thus, the equation above reduces to:

$$\frac{\Delta[\text{GFP}]}{\Delta[\text{RFP}]} = \frac{(\kappa_1\kappa_3 B_1 B_3+\varepsilon_3(\kappa_1 B_1 B_3 n_3+\kappa_1 B_1 X A_3 n_3))(\varepsilon_2'-\varepsilon_2)+(\kappa_3 B_1 B_3 n_1+\kappa_3 B_3 X A_1 n_1)(\varepsilon_1\varepsilon_2'-\varepsilon_1'\varepsilon_2)}{(\kappa_2\kappa_3 B_2 B_3+\varepsilon_3(\kappa_2 B_2 B_3 n_3+\kappa_3 B_3 X A_2 n_3))(\varepsilon_1'-\varepsilon_1)-(\kappa_3 B_2 B_3 n_2+\kappa_3 B_3 X A_2 n_2)(\varepsilon_1\varepsilon_2'-\varepsilon_1'\varepsilon_2)}$$

Or lumping the constant terms, we have

$$\frac{\Delta[\text{GFP}]}{\Delta[\text{RFP}]} = \frac{K_1(\varepsilon_2'-\varepsilon_2)+K_2(\varepsilon_1\varepsilon_2'-\varepsilon_1'\varepsilon_2)}{K_3(\varepsilon_1'-\varepsilon_1)-K_4(\varepsilon_1\varepsilon_2'-\varepsilon_1'\varepsilon_2)} \quad (32)$$

Since the relationship between ε_2 and ε_1 is linear (Figure S4), substituting a linear form ($\varepsilon_2 = A + B\varepsilon_1$) into Equation 32 leads to a linear expression for the slope ($\frac{K_1 B - K_2 A}{K_3 - K_4 A}$). Thus, the coupling correlation in System 2 is linear.

System #3

1. Circuit 1 is identical to that of System #1.

2. Circuit 2

In this circuit, aTc (C_{TR}) is the inducer for the pTet* promoter controlling the expression of the regulators InvF and SicA. As described above, the activation of the pTet* promoter by aTc is similar to that of System #2. $[InvF]_0$, $[SicA]_0$, [InvF], and [SicA] represent the concentration of the total InvF, total SicA, free InvF, and free SicA in the system, respectively. Here, transcriptional parameters for the InvF-SicA operon are shown with subscript 3 while translational parameters are with 4 and 5 for InvF and SicA, respectively (e.g., the mRNAs coding for InvF and SicA are denoted by m_4 and m_5, respectively). Transcriptional and translational parameters for GFP are shown with subscript 2. The 1:2 complex of InvF and SicA (C_{IS}) is the activator for GFP expression. All parameters have the same meaning as defined earlier.

***Transcriptional reactions*:**

$$C_{TR} + b_3^* \underset{\mu_3^-}{\overset{\mu_3^+}{\leftrightarrow}} b_3, \quad b_3 + x \underset{\kappa_3^-}{\overset{\kappa_3^+}{\leftrightarrow}} c_3, \quad c_3 \xrightarrow{\gamma_3} b_3 + x + m_4 + m_5, \quad m_4 \xrightarrow{\delta_4} \varnothing, \quad m_5 \xrightarrow{\delta_5} \varnothing,$$

$$C_{IS} + b_2^* \underset{\mu_2^-}{\overset{\mu_2^+}{\leftrightarrow}} b_2, \quad b_2 + x \underset{\kappa_2^-}{\overset{\kappa_2^+}{\leftrightarrow}} c_2, \quad c_2 \xrightarrow{\gamma_2} b_2 + x + m_2, \quad m_2 \xrightarrow{\delta_2} \varnothing$$

***Activator complex formation*:**

$$[InvF] + 2[SicA] \underset{\kappa_{IS}^-}{\overset{\kappa_{IS}^+}{\leftrightarrow}} C_{IS}$$

***Translational reactions*:**

$$m_i + y \underset{k_i^-}{\overset{k_i^+}{\leftrightarrow}} d_i \xrightarrow{a_i\delta_i} y \qquad i \in \{2,4,5\}$$

$$d_2 \xrightarrow{\pi_2} m_2 + y + [GFP], \qquad [GFP] \xrightarrow{\lambda_2} \varnothing$$

$$d_4 \xrightarrow{\pi_4} m_4 + y + [InvF]_0, \qquad [InvF]_0 \xrightarrow{\lambda_4} \varnothing$$

$$d_5 \xrightarrow{\pi_5} m_5 + y + [SicA]_0, \qquad [SicA]_0 \xrightarrow{\lambda_5} \varnothing$$

***ODE models*:**

$$\frac{db_2}{dt} = \left(\mu_2^+ C_{IS} b_2^* - \mu_2^- b_2\right) - \left(\kappa_2^+ x b_2 - \kappa_2^- c_2\right) + \gamma_2 c_2 \tag{33}$$

$$\frac{db_3}{dt} = \left(\mu_3^+ C_{TR} b_3^* - \mu_3^- b_3\right) - \left(\kappa_3^+ x b_3 - \kappa_3^- c_3\right) + \gamma_3 c_3 \tag{34}$$

$$\frac{dC_{IS}}{dt} = \kappa_{IS}^+ [InvF][SicA]^2 - \kappa_{IS}^- C_{IS} \tag{35}$$

$$\frac{dc_3}{dt} = \left(\kappa_3^+ x b_3 - \kappa_3^- c_3\right) - \gamma_3 c_3 \tag{36}$$

$$\frac{dm_2}{dt} = \gamma_2 c_2 - \delta_2 m_2 - \left(k_2^+ m_2 y - k_2^- d_2\right) + \pi_2 d_2, \tag{37}$$

$$\frac{dm_i}{dt} = \gamma_i c_3 - \delta_i m_i - \left(k_i^+ m_i y - k_i^- d_i\right) + \pi_i d_i, \quad i \in \{4,5\} \tag{38-39}$$

$$\frac{dd_i}{dt} = \left(k_i^+ m_i y - k_i^- d_i\right) - \pi_i d_i - a_i \delta_i d_i, \; i \in \{2,4,5\} \tag{40-42}$$

$$\frac{d[GFP]}{dt} = \pi_2 d_2 - \lambda_2 [GFP] \tag{43}$$

$$\frac{d[InvF]_0}{dt} = \pi_4 d_4 - \lambda_4 [InvF]_0 \tag{44}$$

$$\frac{d[SicA]_0}{dt} = \pi_5 d_5 - \lambda_5 [SicA]_0 \tag{45}$$

***Mass balances*:**

The mass balances for the different plasmids, RNAP, and ribosome are shown below. We also have mass balances for InvF and SicA. $[InvF]_0$, $[SicA]_0$, InvF, and SicA are the concentration of total InvF, total SicA, free InvF, and free SicA, respectively.

$$n_i = b_i^* + b_i + c_i, \quad i \in \{1,2,3\} \text{ (Plasmids 1, 2, and 3 are p15A, ColE1, and pSC101, respectively)} \qquad (46\text{-}48)$$

$$X = x + \sum c_i \ (i=1,2,3) \qquad (49)$$

$$Y = y + \sum d_i \ (i=1,2,4,5) \qquad (50)$$

$$[InvF]_0 = [InvF] + b_2 + C_{IS} \qquad (51)$$

$$[SicA]_0 = [SicA] + 2b_2 + 2C_{IS} \qquad (52)$$

A similar analysis as in System #2 yields

$$\frac{\Delta[GFP]}{\Delta[RFP]} = \frac{\left(\kappa_1\kappa_3 B_1B_4B_5 + \varepsilon_3(\kappa_1 B_1B_4B_5n_3 + \kappa_1 B_1B_5XA_4n_3 + \kappa_3 B_1B_4XA_5n_3)\right)(\varepsilon_2' - \varepsilon_2) + \left(\kappa_3 B_1B_4B_5n_1 + \kappa_3 B_4B_5XA_1n_1\right)(\varepsilon_1\varepsilon_2' - \varepsilon_1'\varepsilon_2)}{\left(\kappa_2\kappa_3 B_2B_4B_5 + \varepsilon_3(\kappa_2 B_2B_4B_5n_3 + \kappa_3 B_4B_5XA_2n_3 + \kappa_3 B_1B_4XA_5n_3)\right)(\varepsilon_1' - \varepsilon_1) - (\kappa_3 B_2B_4B_5n_2 + \kappa_3 B_4B_5XA_2n_2)(\varepsilon_1\varepsilon_2' - \varepsilon_1'\varepsilon_2)}$$

Lumping the constant terms, we have

$$\frac{\Delta[GFP]}{\Delta[RFP]} = \frac{K_5(\varepsilon_2' - \varepsilon_2) + K_6(\varepsilon_1\varepsilon_2' - \varepsilon_1'\varepsilon_2)}{K_7(\varepsilon_1' - \varepsilon_1) - K_8(\varepsilon_1\varepsilon_2' - \varepsilon_1'\varepsilon_2)} \qquad (53)$$

In this case, the relationship between ε_2 and ε_1 is nonlinear (Figure S4), giving us a changing slope. Thus, the coupling correlation in System 3 is non-linear (see also Section [2]).

System #2 (Negative Feedback)

1. Circuit 1 is identical to that of System #1.

2. Circuit 2

In this circuit, aTc (C_{TR}) is the inducer for the pTet* promoter controlling the expression of the transcription factor ExsA. C_{TR} activates the pTet* promoter (b_3) by binding the TetR repressor that is initially in the TetR-pTet* complex (b_3^*). $[ExsA]_0$ and [ExsA] represent the total and the free ExsA concentration in the system, respectively. ExsA is the activator for both GFP and ExsD expression. In addition, ExsA and ExsD can form a complex that is not able to activate GFP and ExsD expression. $[ExsD]_0$ and [ExsD] represent the total and the

free ExsD concentration, respectively. Here, transcription and translation parameters for ExsA are shown with subscript 3, while those of ExsD and GFP are with *d* and 2, respectively. All parameters have the same meaning as defined earlier.

***Trascriptional reactions*:**

$$C_{TR} + b_3^* \underset{\mu_3^-}{\overset{\mu_3^+}{\leftrightarrow}} b_3, \quad b_3 + x \underset{\kappa_3^-}{\overset{\kappa_3^+}{\leftrightarrow}} c_3, \quad c_3 \xrightarrow{\gamma_3} b_3 + x + m_3, \quad m_3 \xrightarrow{\delta_3} \varnothing$$

$$[\text{ExsA}] + b_2^* \underset{\mu_2^-}{\overset{\mu_2^+}{\leftrightarrow}} b_2, \quad b_2 + x \underset{\kappa_2^-}{\overset{\kappa_2^+}{\leftrightarrow}} c_2, \quad c_2 \xrightarrow{\gamma_2} b_2 + x + m_2 + m_d, \quad m_2 \xrightarrow{\delta_2} \varnothing, m_d \xrightarrow{\delta_d} \varnothing$$

***Translational reactions*:**

$$m_3 + y \underset{k_3^-}{\overset{k_3^+}{\leftrightarrow}} d_3 \xrightarrow{a_3\delta_3} y, \quad d_3 \xrightarrow{\pi_3} m_3 + y + [\text{ExsA}]_0, \quad [\text{ExsA}]_0 \xrightarrow{\lambda_3} \varnothing$$

$$m_2 + y \underset{k_2^-}{\overset{k_2^+}{\leftrightarrow}} d_2 \xrightarrow{a_2\delta_2} y, \quad d_2 \xrightarrow{\pi_2} m_2 + y + [\text{GFP}], \quad [\text{GFP}] \xrightarrow{\lambda_2} \varnothing$$

$$m_d + y \underset{k_d^-}{\overset{k_d^+}{\leftrightarrow}} d_d \xrightarrow{a_d\delta_d} y, \quad d_d \xrightarrow{\pi_d} m_d + y + [\text{ExsD}]_0, \quad [\text{ExsD}]_0 \xrightarrow{\lambda_d} \varnothing$$

***Interaction of ExsA and ExsD*:**

$$[\text{ExsA}] + [\text{ExsD}] \underset{}{\overset{K_{AD}}{\leftrightarrow}} [\text{ExsA-ExsD}]$$

***ODE models*:**

$$\frac{db_2}{dt} = \left(\mu_2^+ [\text{ExsA}] b_2^* - \mu_2^- b_2\right) - \left(\kappa_2^+ x b_2 - \kappa_2^- c_2\right) + \gamma_2 c_2, \tag{54}$$

$$\frac{db_3}{dt} = \left(\mu_3^+ C_{TR} b_3^* - \mu_3^- b_3\right) - \left(\kappa_3^+ x b_3 - \kappa_3^- c_3\right) + \gamma_3 c_3, \tag{55}$$

$$\frac{dc_i}{dt} = \left(\kappa_i^+ x b_i - \kappa_i^- c_i\right) - \gamma_i c_i, \qquad i \in \{2,3\} \tag{56-57}$$

$$\frac{dm_i}{dt} = \gamma_i c_i - \delta_i m_i - (k_i^+ m_i y - k_i^- d_i) + \pi_i d_i, \quad i \in \{2,3\} \tag{58-59}$$

$$\frac{dm_d}{dt} = \gamma_2 c_2 - \delta_d m_d - (k_d^+ m_d y - k_d^- d_d) + \pi_d d_d \tag{60}$$

$$\frac{dd_i}{dt} = \left(k_i^+ m_i y - k_i^- d_i\right) - \pi_i d_i - a_i \delta_i d_i, \; i \in \{2,3\} \tag{61-62}$$

$$\frac{dd_d}{dt} = (k_d^+ m_d y - k_d^- d_d) - \pi_d d_d - a_d \delta_d d_d \tag{63}$$

$$\frac{d[\text{ExsA}]_0}{dt} = \pi_3 d_3 - \lambda_3 [\text{ExsA}]_0 . \tag{64}$$

$$\frac{d[\text{ExsD}]_0}{dt} = \pi_d d_d - \lambda_d [\text{ExsD}]_0 \tag{65}$$

$$\frac{d[\text{GFP}]}{dt} = \pi_2 d_2 - \lambda_2 [\text{GFP}]. \tag{66}$$

***Mass balances*:**

We can write similar mass balances as in System #2 for the different plasmids, RNAP, and ribosome.

$n_i = b_i^* + b_i + c_i$, $i \in \{1,2,3\}$ (Plasmids 1, 2, and 3 are p15A, ColE1, and pSC101, respectively) (67-69)

$$X = x + \sum_{i=1}^{3} c_i \tag{70}$$

$$Y = y + \sum_{i=1}^{3} d_i + d_d \tag{71}$$

$[\text{ExsA}]_0 = [\text{ExsA}] + b_2 + [\text{ExsA-ExsD}]$ (72)

$[\text{ExsD}]_0 = [\text{ExsD}] + [\text{ExsA-ExsD}]$ (73)

[2] Mathematical analysis to determine resource-coupling correlations in systems with three different circuit topologies - numerical solution

To validate mathematical analyses above, we performed numerical simulations for Systems #1, 2, and 3. To numerically solve for varibles, we assumed steady-state conditions for the same ODEs as described above.

Based on previous reports (2-4), the following Hill coefficients were used: 2 (pLux*), 2 (pCI), 2 (pTet*), 1 (pexsD), and 1 (psicA). Parameter values used in our simulations are summarized in Table S2.

Equations used for numerical simulations:

- **System #1 (Open Loop):** Same as described above. Variables to be solved are *x*, *y*, [RFP], and [GFP].

- **System #2 (Open Loop):** Variables to be solved are *x*, *y*, [RFP], [GFP], and [ExsA].

1	$x+\xi_1 n_1 \frac{x}{x+\kappa_1}+\xi_2 n_2 \frac{x}{x+\kappa_2}+\xi_3 n_3 \frac{x}{x+\kappa_3}-X=0$
2	$y+\xi_1 \frac{\gamma_1 n_1}{\delta_1} \frac{x}{x+\kappa_1} \frac{y}{y+k_1}+\xi_2 \frac{\gamma_2 n_2}{\delta_2} \frac{x}{x+\kappa_2} \frac{y}{y+k_2}+\xi_3 \frac{\gamma_3 n_3}{\delta_3} \frac{x}{x+\kappa_3} \frac{y}{y+k_3}-Y=0$
3	$\xi_1 \frac{\pi_1}{\lambda_1} \frac{\gamma_1 n_1}{\delta_1} \frac{x}{x+\kappa_1} \frac{y}{y+k_1}-[\mathrm{RFP}]=0$
4	$\xi_2 \frac{\pi_2}{\lambda_2} \frac{\gamma_2 n_2}{\delta_2} \frac{x}{x+\kappa_2} \frac{y}{y+k_2}-[\mathrm{GFP}]=0$
5	$\xi_3 \frac{\pi_3}{\lambda_3} \frac{\gamma_3 n_3}{\delta_3} \frac{x}{x+\kappa_3} \frac{y}{y+k_3}-\left([\mathrm{ExsA}]+\kappa_2 \xi_2 n_2 \frac{1}{x+\kappa_2}\right)=0$

where $\xi_1=\frac{[3\mathrm{OC6}]^2}{[3\mathrm{OC6}]^2+K_{u1}}$, $\xi_2=\frac{[\mathrm{ExsA}]}{[\mathrm{ExsA}]+K_{p1}}$, and $\xi_3=\frac{[\mathrm{aTc}]^2}{[\mathrm{aTc}]^2+K_{u2}}$.

- **System #2 (Negative Feedback):** Variables to be solved are *x*, *y*, [RFP], [GFP], [ExsA], and [ExsD].

1	$x+\xi_1 n_1 \frac{x}{x+\kappa_1}+\xi_2 n_2 \frac{x}{x+\kappa_2}+\xi_3 n_3 \frac{x}{x+\kappa_3}-X=0$
2	$y+\xi_1 \frac{\gamma_1 n_1}{\delta_1} \frac{x}{x+\kappa_1} \frac{y}{y+k_1}+\xi_2 \frac{\gamma_2 n_2}{\delta_2} \frac{x}{x+\kappa_2} \frac{y}{y+k_2}+\xi_2 \frac{\gamma_2 n_2}{\delta_d} \frac{x}{x+\kappa_2} \frac{y}{y+k_d}$ $+\xi_3 \frac{\gamma_3 n_3}{\delta_3} \frac{x}{x+\kappa_3} \frac{y}{y+k_3}-Y=0$
3	$\xi_1 \frac{\pi_1}{\lambda_1} \frac{\gamma_1 n_1}{\delta_1} \frac{x}{x+\kappa_1} \frac{y}{y+k_1}-[\mathrm{RFP}]=0$

4	$\xi_2 \frac{\pi_2}{\lambda_2} \frac{\gamma_2 n_2}{\delta_2} \frac{x}{x+\kappa_2} \frac{y}{y+k_2} - [\text{GFP}] = 0$
5	$\xi_3 \frac{\pi_3}{\lambda_3} \frac{\gamma_3 n_3}{\delta_3} \frac{x}{x+\kappa_3} \frac{y}{y+k_3} - \left([\text{ExsA}] + \kappa_2 \xi_2 n_2 \frac{1}{x+\kappa_2} + \frac{[\text{ExsA}][\text{ExsD}]}{K_{\text{AD}}} \right) = 0$
6	$\xi_2 \frac{\pi_d}{\lambda_d} \frac{\gamma_2 n_2}{\delta_d} \frac{x}{x+\kappa_2} \frac{y}{y+k_d} - \left([\text{ExsD}] + \frac{[\text{ExsA}][\text{ExsD}]}{K_{\text{AD}}} \right) = 0$

where $\xi_1 = \frac{[3\text{OC6}]^2}{[3\text{OC6}]^2 + K_{u1}}$, $\xi_2 = \frac{[\text{ExsA}]}{[\text{ExsA}] + K_{p1}}$, and $\xi_3 = \frac{[\text{aTc}]^2}{[\text{aTc}]^2 + K_{u2}}$.

- **System #3 (Open Loop):** Variables to be solved are *x*, *y*, [RFP], [GFP], [InvF] and [SicA].

1	$x + \xi_1 n_1 \frac{x}{x+\kappa_1} + \xi_2 n_2 \frac{x}{x+\kappa_2} + \xi_3 n_3 \frac{x}{x+\kappa_3} - X = 0$
2	$y + \xi_1 \frac{\gamma_1 n_1}{\delta_1} \frac{x}{x+\kappa_1} \frac{y}{y+k_1} + \xi_2 \frac{\gamma_2 n_2}{\delta_2} \frac{x}{x+\kappa_2} \frac{y}{y+k_2} + \xi_3 \frac{\gamma_3 n_3}{\delta_4} \frac{x}{x+\kappa_3} \frac{y}{y+k_4}$ $+ \xi_3 \frac{\gamma_3 n_3}{\delta_5} \frac{x}{x+\kappa_3} \frac{y}{y+k_5} - Y = 0$
3	$\xi_1 \frac{\pi_1}{\lambda_1} \frac{\gamma_1 n_1}{\delta_1} \frac{x}{x+\kappa_1} \frac{y}{y+k_1} - [\text{RFP}] = 0$
4	$\xi_2 \frac{\pi_2}{\lambda_2} \frac{\gamma_2 n_2}{\delta_2} \frac{x}{x+\kappa_2} \frac{y}{y+k_2} - [\text{GFP}] = 0$
5	$\xi_3 \frac{\pi_4}{\lambda_4} \frac{\gamma_3 n_3}{\delta_4} \frac{x}{x+\kappa_3} \frac{y}{y+k_4} - \left([\text{InvF}] + \kappa_2 \xi_2 n_2 \frac{1}{x+\kappa_2} + \frac{[\text{InvF}][\text{SicA}]^2}{K_{\text{IS}}} \right) = 0$
6	$\xi_3 \frac{\pi_5}{\lambda_5} \frac{\gamma_3 n_3}{\delta_5} \frac{x}{x+\kappa_3} \frac{y}{y+k_5} - \left([\text{SicA}] + 2\kappa_2 \xi_2 n_2 \frac{1}{x+\kappa_2} + 2\frac{[\text{InvF}][\text{SicA}]^2}{K_{\text{IS}}} \right) = 0$

where $\xi_1 = \frac{[3\text{OC6}]^2}{[3\text{OC6}]^2 + K_{u1}}$, $\xi_2 = \frac{\frac{[\text{InvF}][\text{SicA}]^2}{K_{\text{IS}}}}{\frac{[\text{InvF}][\text{SicA}]^2}{K_{\text{IS}}} + K_{p2}}$, and $\xi_3 = \frac{[\text{aTc}]^2}{[\text{aTc}]^2 + K_{u2}}$.

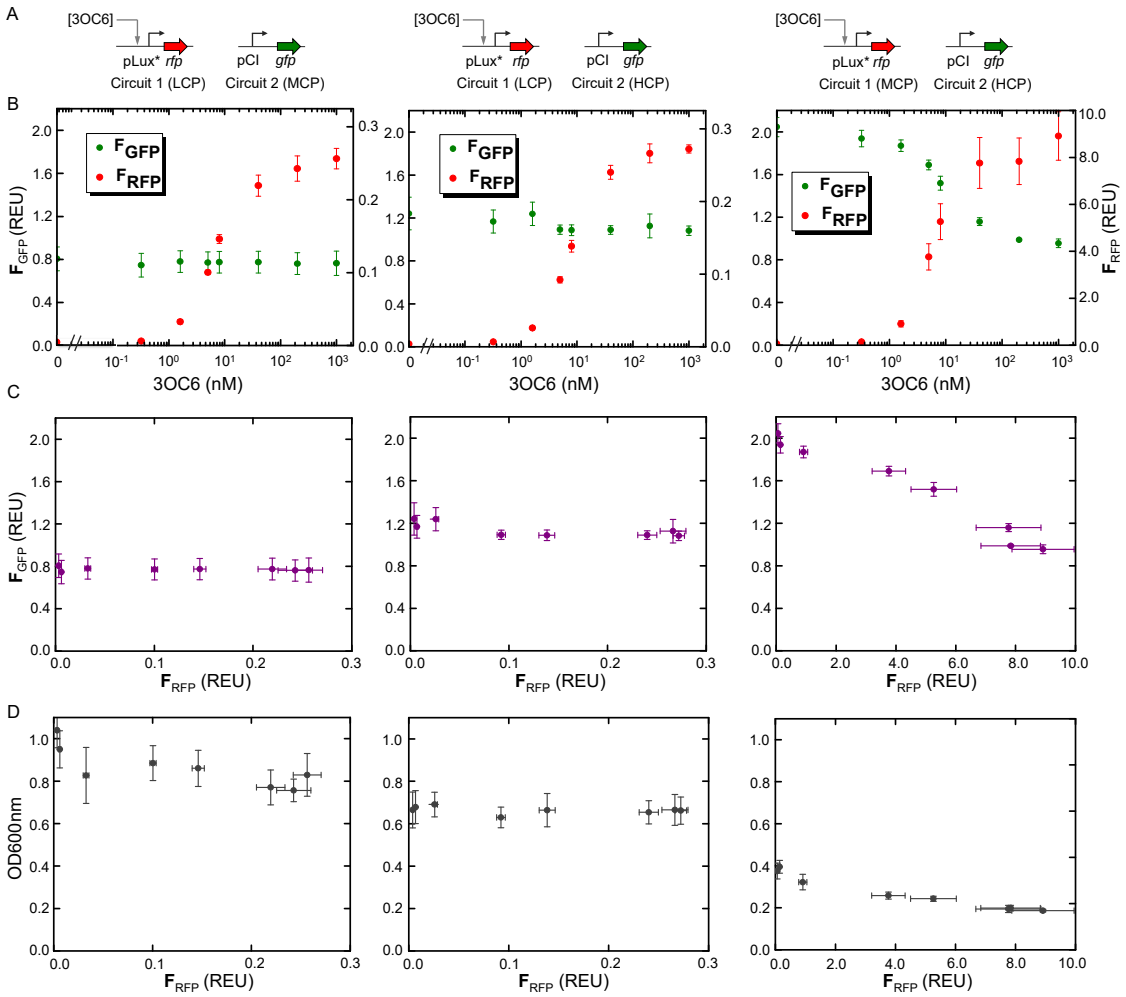

Supplementary Figure S1. Effect of plasmid copy numbers on resource-coupled interference between independent genetic circuits. A. Schematic diagrams of System 1 as shown in Figure 1. Three subsystems were constructed with various combinations of plasmid copy numbers. LCP, MCP, and HCP represent low, medium, and high copy plasmid, respectively. An inducible promoter (pLux*) controls RFP expression while GFP is constitutively expressed from the pCI promoter. **B.** Competition for limited resources couples independent circuits. RFP expression (by adding 3OC6) is strongly coupled with GFP expression only when a combination of MCP and HCP is used for Circuits 1 and 2, respectively. F_{GFP} (left y-axis) and F_{RFP} (right y-axis). Note that the RFP expression range is different for the figure in the right panel (the MCP-HCP combination). For the pLux* promoter, pLux*_-35N4G was used in all three systems (Table S6). The experiments were performed at 3OC6 concentrations of 0, 0.32, 1.6, 5, 8, 40, 200, and 1,000 nM. **C**. Relationship between RFP and GFP expression. A combination of LCP and MCP generates no correlation (R^2 = 0.133, P > 0.05), LCP and HCP generates a weak correlation (R^2 = 0.504, P < 0.05), and MCP and HCP generates a strong linear coupling correlation (R^2 = 0.974, P < 0.001) determined using linear least squares method. Data were fitted to an equation $F_{GFP} = a - b\,F_{RFP}$. The data and error bars show the average and s.e.m of at least three biological replicates performed on different days. **D.** $OD600_{nm}$ plotted against F_{RFP}. Absorbance (Abs) values obtained from the plate reader were converted into $OD600_{nm}$ by using the equation ($OD600_{nm}$ = 1.6446 × Abs + 0.0138) that was experimentally determined. The data and error bars show the average and s.e.m of at least three biological replicates performed on different days.

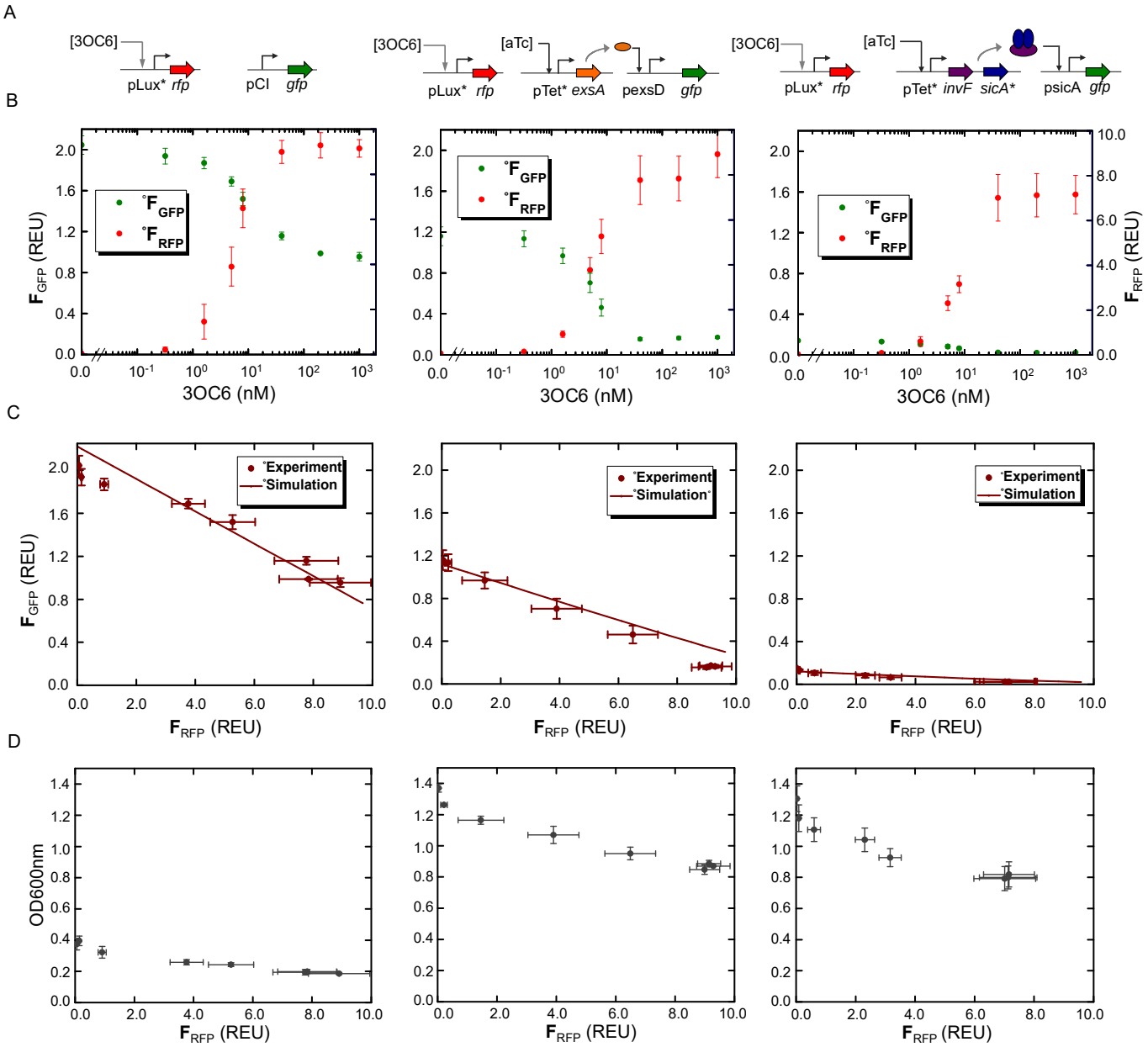

<u>Supplementary Figure S2</u>. Plots on the same scale axes and $OD600_{nm}$ data for Figure 2. A. Schematic diagrams of genetic circuits as shown in Figure 1. **B.** Plots on the same scale axes (Figure 2B) for comparison between Systems 1, 2, and 3. **C.** Plots on the same scale axes (Figure 2C) for comparison between Systems 1, 2, and 3. **D.** $OD600_{nm}$ plotted against F_{RFP} (REU) in Systems 1, 2, and 3. Absorbance (Abs) values obtained from the plate reader were converted into $OD600_{nm}$ by using the equation ($OD600_{nm}$ = 1.6446 × Abs + 0.0138) that was experimentally determined. The experiments were performed at 3OC6 concentrations of 0, 0.32, 1.6, 5, 8, 40, 200, and 1,000 nM and an aTc concentration of 0 (System 1) or 50 ng/ml (Systems 2 and 3). The data and error bars show the average and s.e.m. of at least three biological replicates performed on different days.

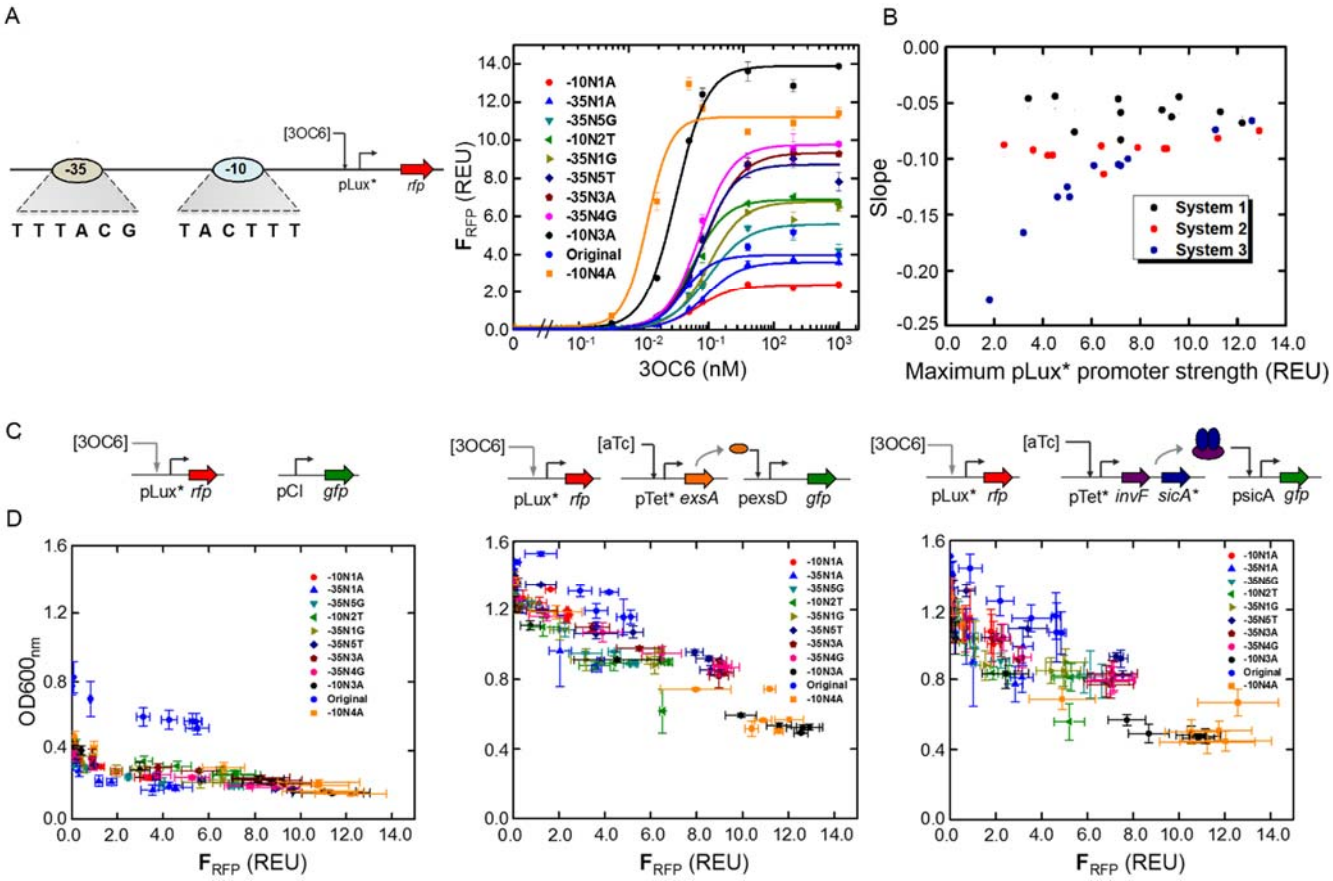

Supplementary Figure S3. Effect of point mutations in the pLux* promoter on resource coupling. A. Building a promoter library by introducing point mutations in the -35 or -10 region. The schematic diagram of the pLux* promoter (Original) is shown in the left panel (2). Ten promoter variants were created by replacing a single nucleotide either in the -35 or -10 region. For example, the notation -10N1A means that the first base in the -10 region was replaced with nucleotide A (from TACTTT to AACTTT). This also applies to the -35 region (e.g., -35N4G from TTTACG to TTTGCG). The right panel shows transfer functions of the promoter variants with parameters shown in Table S3. The experiments were performed at 3OC6 concentrations of 0, 0.32, 1.6, 5, 8, 40, 200, and 1,000 nM. **B.** Linear regression analysis of experimental data shows that the slope of the coupling correlation is independent of the pLux* promoter strength for System 1 (R^2 = -0.07, P > 0.05) and System 2 (R^2 = 0.179, P > 0.05). In contrast, the slope increases with the pLux* promoter strength in System 3 (R^2 = 0.793, P < 0.001). **C.** Schematic diagrams of genetic circuits shown in Figure 1. **D.** $OD600_{nm}$ plotted against F_{RFP} (REU) in Systems 1, 2, and 3 (for Figure 3B). Absorbance (Abs) values obtained from the plate reader were converted into $OD600_{nm}$ by using the equation ($OD600_{nm}$ = 1.6446 × Abs + 0.0138) that was experimentally determined. The data and error bars show the average and s.e.m. of at least three biological replicates performed on different days.

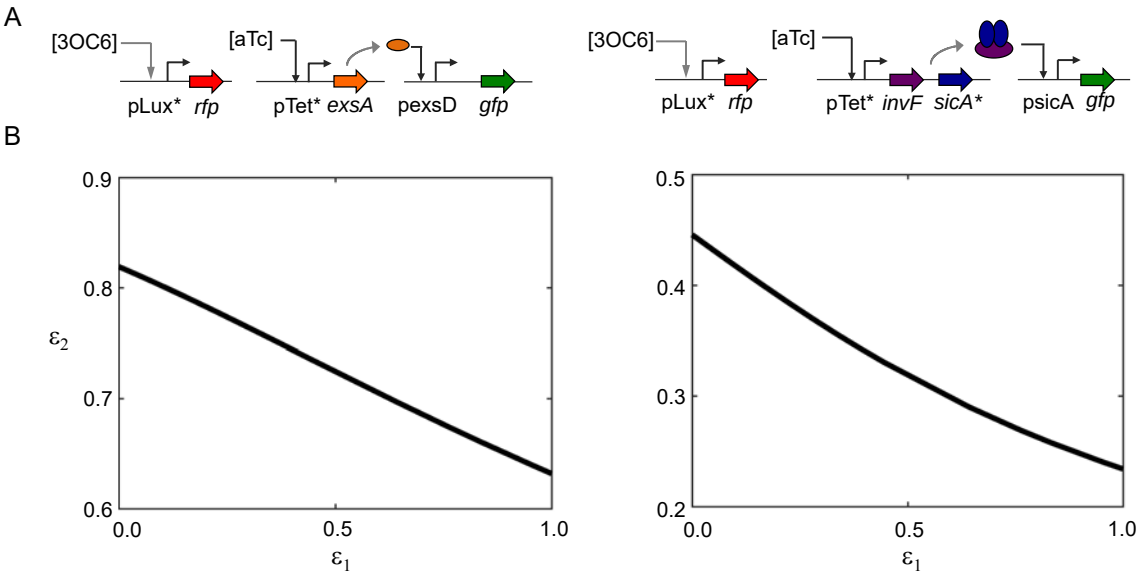

Supplementary Figure S4. Relationship between ε_1 and ε_2 in Systems 2 and 3. A. Schematic diagrams of genetic circuits in Systems 2 and 3. **B.** Numerical simulations showing linear and non-linear ε_1–ε_2 relationships for Systems 2 and 3, respectively. ε_1 and ε_2 are defined in Box 1. Simulations were done using 3OC6 concentrations of 0 – 1,000 nM. The other parameters used for these simulations are shown in Table S2.

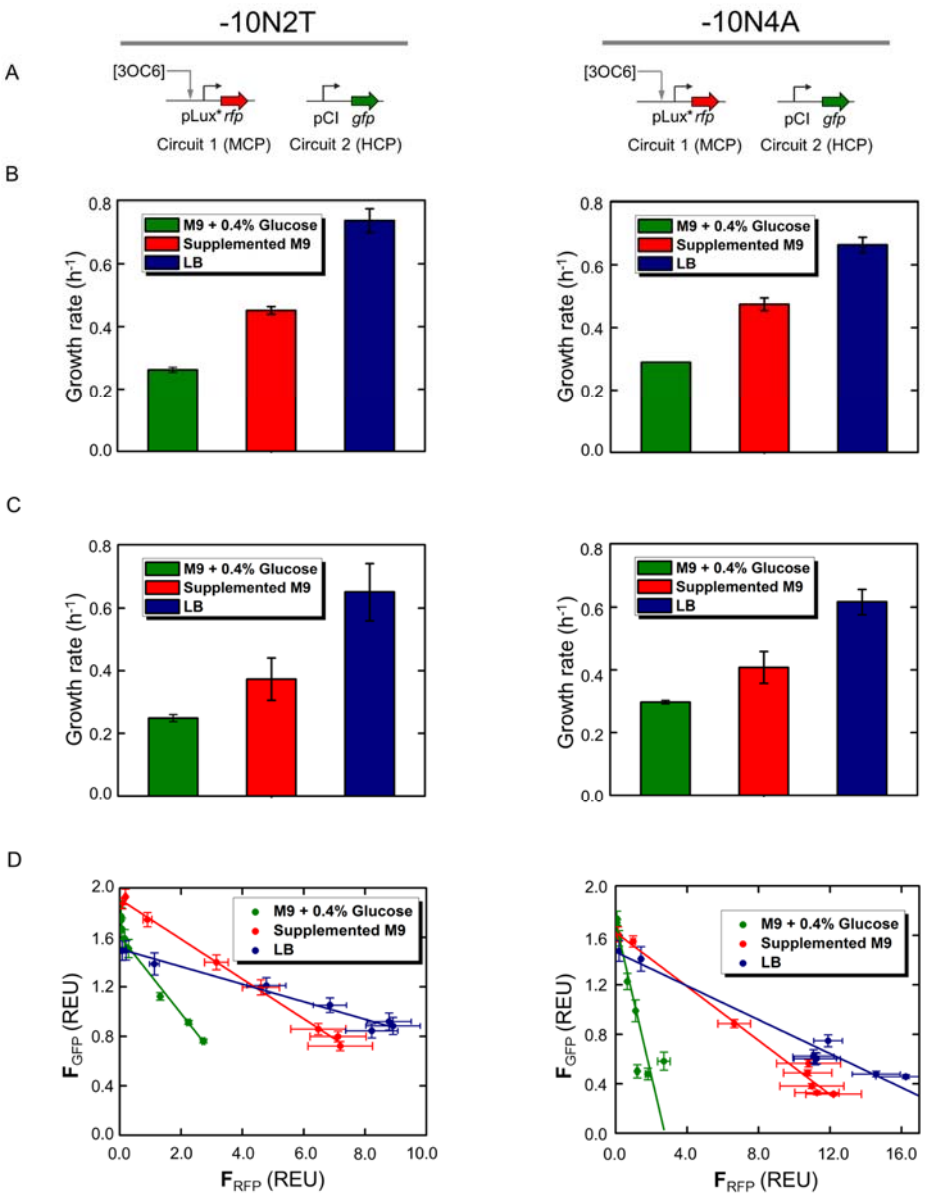

Supplementary Figure S5. Effects of different growth media on growth rates and the coupling correlation. Three different media were used as described in the Methods section: M9 + 0.4% glucose; supplemented M9; and LB. **A.** Schematic diagrams of System 1. Left, System 1 with a pLux* variant (-10N2T; Table S3). Right, System 1 with a pLux* variant (-10N4A; Table S3). **B.** Specific growth rates measured at 0 nM 3OC6. **C.** Specific growth rates measured at 1,000 nM 3OC6. **D.** Coupling correlation. The experimental data were fitted to an equation $F_{GFP} = a - bF_{RFP}$ to calculate and compare the slopes between different nutrient conditions. For the left figure, fitted equations are: $F_{GFP} = 1.61 - 0.313\,F_{RFP}$, R^2 = 0.974 (M9 + 0.4% Glucose); $F_{GFP} = 1.91 - 0.161\,F_{RFP}$, R^2 = 0.996 (Supplemented M9); and $F_{GFP} = 1.51 - 0.070\,F_{RFP}$, R^2 = 0.964 (LB). For the right figure, fitted equations are: $F_{GFP} = 1.70 - 0.619\,F_{RFP}$, R^2 = 0.839 (M9 + 0.4% Glucose); $F_{GFP} = 1.62 - 0.110\,F_{RFP}$, R^2 = 0.959 (Supplemented M9); and $F_{GFP} = 1.46 - 0.070\,F_{RFP}$, R^2 = 0.960 (LB). Experiments were performed at 3OC6 concentrations of 0, 0.32, 1.6, 5, 8, 40, 200, and 1,000 nM. The data and error bars show the average and s.e.m. of at least three biological replicates performed on different days.

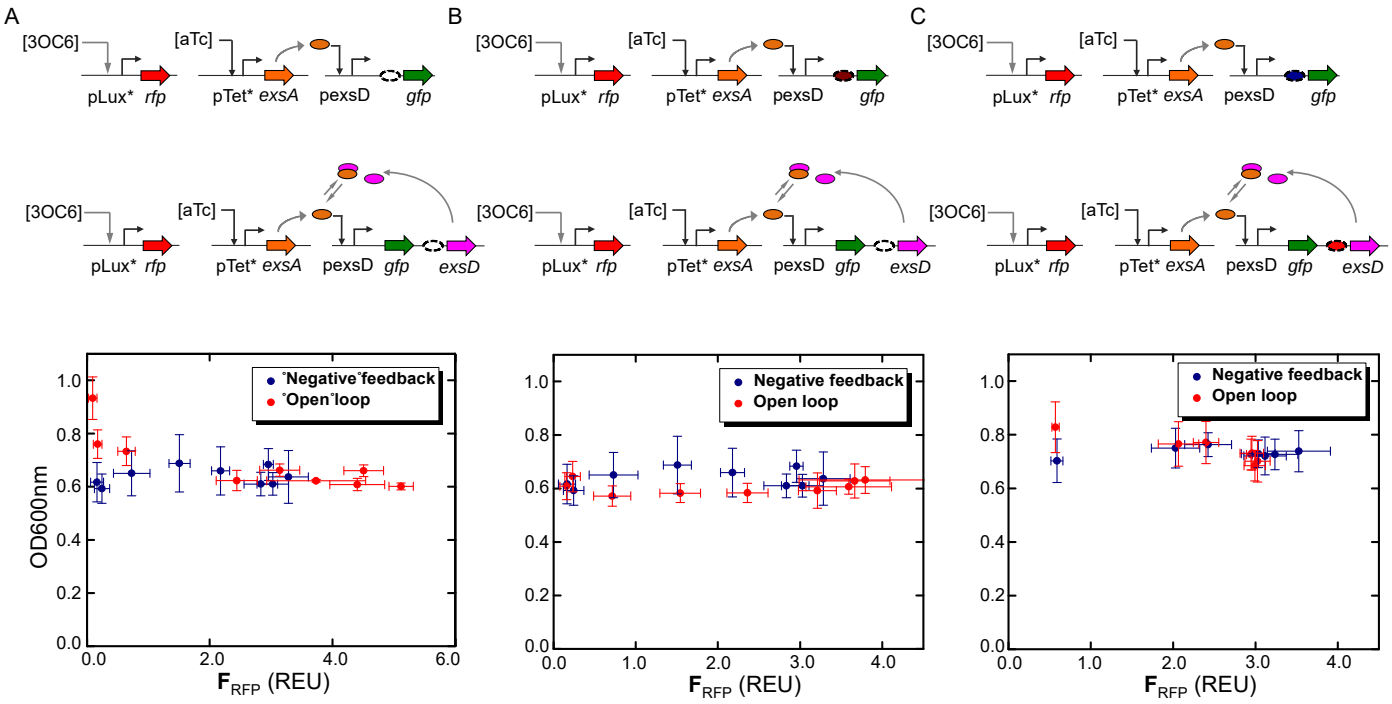

Supplementary Figure S6. $OD600_{nm}$ data for Figure 5. Schematic diagrams shown in this figure are same as those in Figure 5. Absorbance (Abs) values obtained from the plate reader were converted into $OD600_{nm}$ by using the equation ($OD600_{nm}$ = 1.6446 × Abs + 0.0138) that was experimentally determined. The data and error bars show the average and s.e.m of three biological replicates performed on different days. Detailed information regarding plasmids, strains, and sequences of promoters and RBSs in this figure is summarized in Tables S4-S6. **A.** The experiments were performed at 3OC6 concentrations of 0, 0.32, 1.6, 5, 8, 20, 40, 200, and 1,000 nM, and an aTc concentration of 50 ng/ml. **B.** The experiments were performed at 3OC6 concentrations of 0, 0.32, 1.6, 5, 8, 20, 40, 200, and 1,000 nM, and an aTc concentration of 50 ng/ml. **C.** The experiments were performed at 3OC6 concentrations of 1.6, 5, 8, 20, 40, 200, and 1,000 nM, and an aTc concentration of 50 ng/ml.

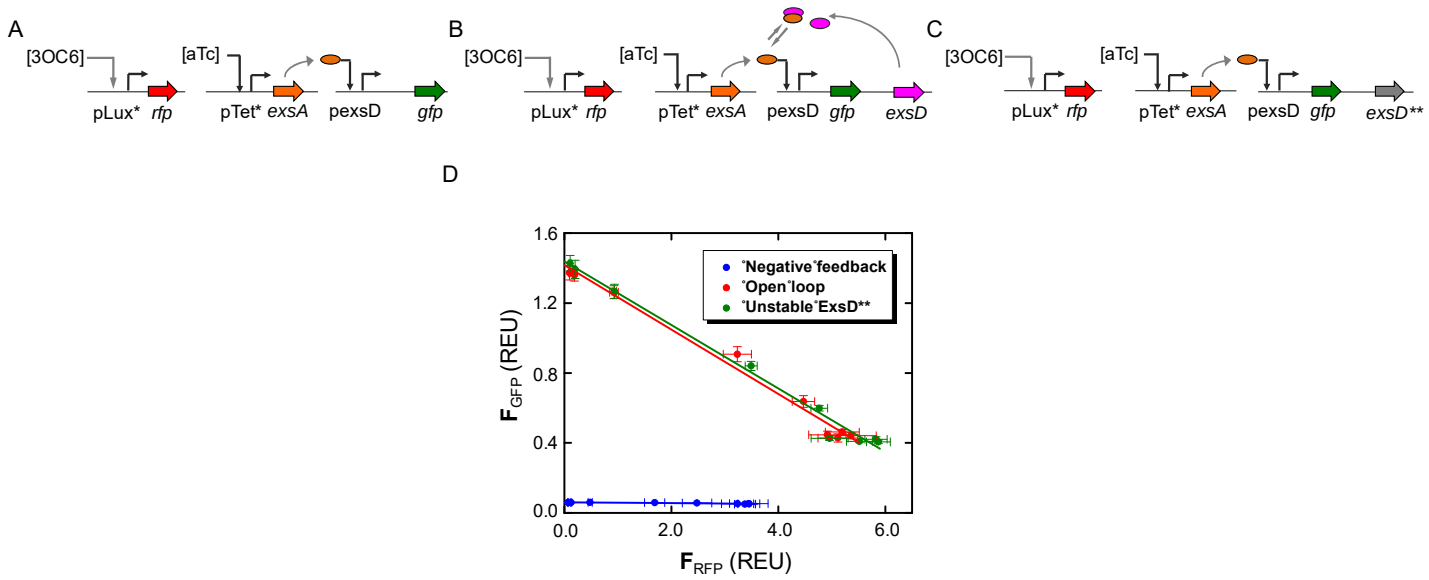

Supplementary Figure S7. An ExsD mutant (ExsD**) that does not reduce GFP expression compared to the open loop counterpart. ExsD** was created by removing ten amino acids from the C-terminal of ExsD, which was reported to make the protein completely unstable (5). **A.** Schematic diagram of an open loop subsystem of System 2. **B.** Schematic diagram of a subsystem of System 2 with a negative feedback loop. **C.** Schematic diagram of a subsystem of System 2 containing ExsD**. **D.** Coupling correlations between GFP and RFP levels. The experimental data were fitted to an equation $F_{GFP} = a - bF_{RFP}$ to calculate and compare the slopes among the three genetic circuits. Fitted equations are: $F_{GFP} = 0.061 - 0.0024\,F_{RFP}$, $R^2 = 0.776$ (Negative feedback; $\beta = 10 \pm 2$); $F_{GFP} = 1.42 - 0.184\,F_{RFP}$, $R^2 = 0.988$ (Open loop; $\beta = 67 \pm 2$); and $F_{GFP} = 1.44 - 0.182\,F_{RFP}$, $R^2 = 0.989$ (Unstable ExsD**; $\beta = 70 \pm 1$). Experiments were performed at 3OC6 concentrations of 0, 0.32, 1.6, 5, 8, 20, 40, 200, and 1,000 nM. Data and error bars are averages and s.e.m. of at least six biological replicates performed on different days.

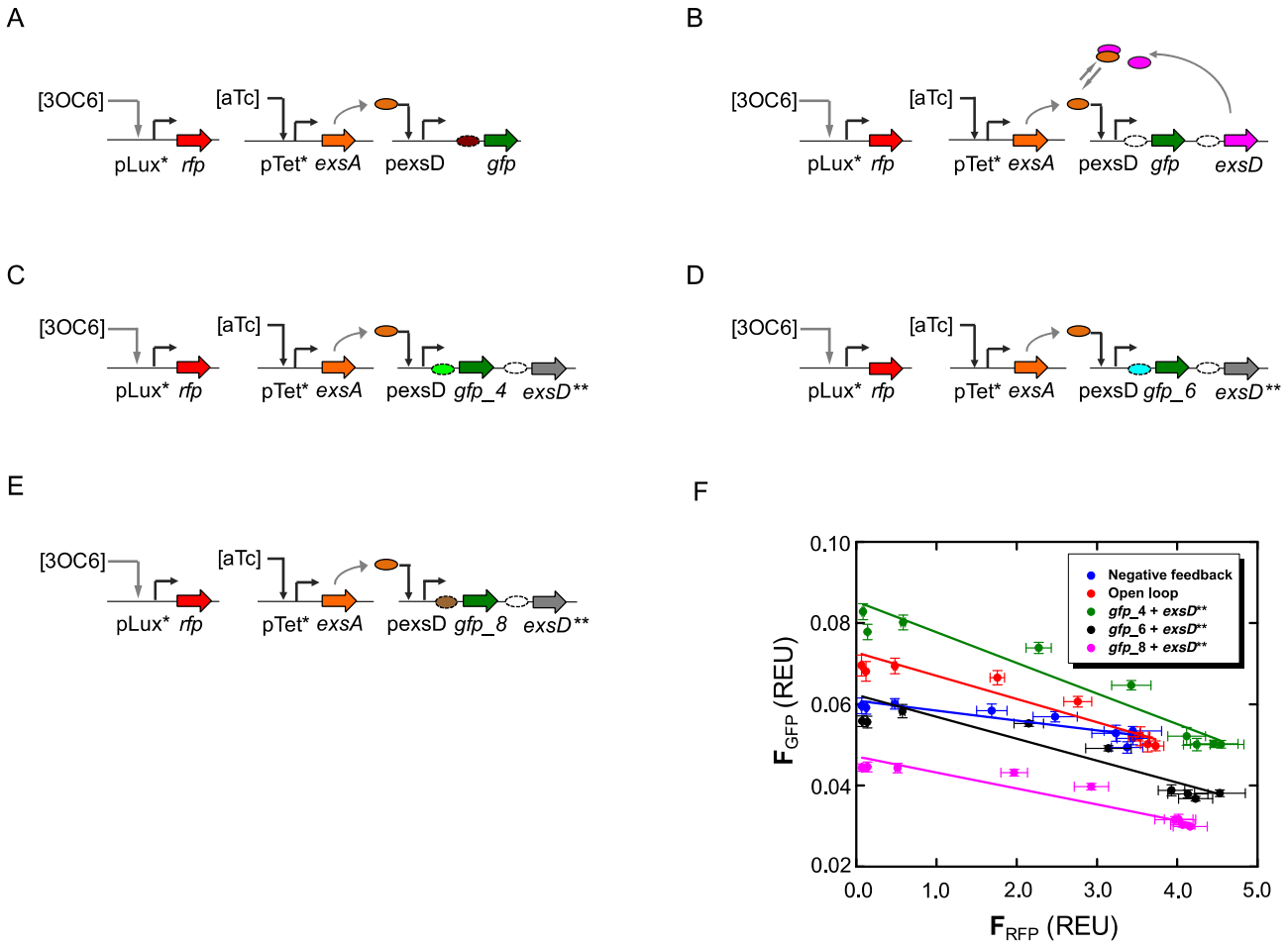

Supplementary Figure S8. Reduced coupling is due to the presence of negative feedback. Three ExsD**-containing subsystems, which have similar GFP levels to that of a negative feedback-containing subsystem or an open loop subsystem, were created by using different ribosome binding site (RBS; dashed oval in the figure) sequences for *gfp* while using the same RBS sequence for ExsD and ExsD**. The changed RBS sequences (6 bases) were indicated below. Detailed information regarding plasmids, strains, and sequences of promoters and RBSs used in this figure is summarized in Supplementary Tables S4-S6. **A.** Schematic diagram of an open loop subsystem of System 2 (RBS changed to TTTGCT). **B.** Schematic diagram of a subsystem of System 2 with a negative feedback loop (original RBS, AGGAGT). **C.** Schematic diagram of a subsystem of System 2 containing ExsD** (RBS changed to CAGGGT; *gfp*_4 + *exsD***). **D.** Schematic diagram of a subsystem of System 2 containing ExsD** (RBS changed to GTAAGT; *gfp*_6 + *exsD***). **E.** Schematic diagram of a subsystem of System 2 containing ExsD** (RBS changed to ATTGTT; *gfp*_8 + *exsD***). **F.** Coupling correlations between GFP and RFP levels. The experimental data were fitted to an equation $F_{GFP} = a - bF_{RFP}$ to calculate and compare the slopes among the five genetic circuits. Fitted equations are: $F_{GFP} = 0.061 - 0.0024\ F_{RFP}$, $R^2 = 0.776$ (Negative feedback; $\beta = 10 \pm 2$); $F_{GFP} = 0.073 - 0.0057\ F_{RFP}$, $R^2 = 0.885$ (Open loop; $\beta = 25 \pm 2$); $F_{GFP} = 0.085 - 0.0075\ F_{RFP}$, $R^2 = 0.909$ (*gfp*_4 + *exsD***; $\beta = 37 \pm 3$); $F_{GFP} = 0.062 - 0.0054\ F_{RFP}$, $R^2 = 0.791$ (*gfp*_6 + *exsD***; $\beta = 31 \pm 2$); and $F_{GFP} = 0.047 - 0.0039\ F_{RFP}$, $R^2 = 0.876$ (*gfp*_8 + *exsD***; $\beta = 29 \pm 2$). Experiments were performed at 3OC6 concentrations of 0, 0.32, 1.6, 5, 8, 20, 40, 200, and 1,000 nM. Data and error bars are averages and s.e.m. of at least six biological replicates performed on different days.

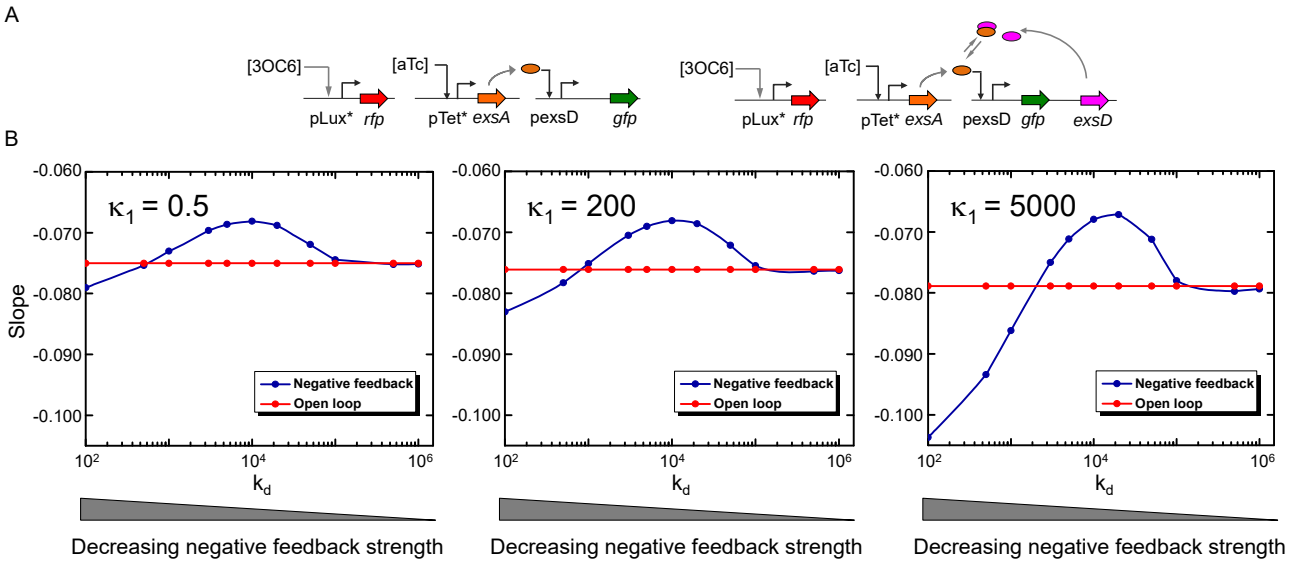

<u>Supplementary Figure S9</u>. Reduction of resource-coupled interference by negative feedback occurs only within a limited range of feedback strength. A. Schematic diagrams of genetic circuits with no negative feedback loop (Open loop; left) and with a negative feedback loop (Negative feedback; right). **B.** Numerical simulations showing the effect of negative feedback strength on the coupling slope. Negative feedback strengths were varied by changing the dissociation constant between *exsD* mRNA and ribosome (k_d) for the negative feedback system. To calculate the slope for F_{GFP}-F_{RFP} coupling correlations, computationally obtained GFP outputs were normalized to their maximum value for each k_d. Numerical simulations were performed using k_d values (nM) of [10^2, 5×10^2, 10^3, 3×10^3, 5×10^3, 10^4, 2×10^4, 5×10^4, 10^5, 5×10^5, 10^6] and the following κ_1 values (nM): 0.5 (left), 200 (middle), and 5,000 (right). Other parameters used in this simulation are shown in Table S2. Too strong (too low k_d) negative feedback can result in more coupling (more negative slope) than the open loop counterpart.

Table S2. Parameter values used in the numerical simulations.

Symbols [a]	System #1	System #2	System #3	References/Notes
k_1	1×10^3	1×10^3	1×10^3	this study [b]
k_2 [c]	1×10^5	1×10^5	1×10^5	(1)
k_3	-	1×10^4	-	(1)
k_4	-	-	1×10^4	(1)
k_5	-	-	1×10^4	(1)
k_d [d]	-	4×10^3	-	(1)
κ_1 [e]	200	200	200	(1)
κ_2	1,000	1,900	17,000	this study [b]
κ_3	-	20	20	(2)
δ_1	10	10	10	(1)
δ_2	10	10	10	(1)

δ_3	-	10	-	(1)
δ_4	-	-	10	(1)
δ_5	-	-	10	(1)
δ_d	-	10	-	(1)
λ_1	1	1	1	(1)
λ_2	1	1	1	(1)
λ_3	-	1	-	(1)
λ_4	-	-	1.3	(6)
λ_5	-	-	2.8	(6)
λ_d	-	0.4	-	this study [b]
π_1	2,700	2,700	2,700	(1)
π_2	2,700	2,700	2,700	(1)
π_3	-	2,700	-	(1)
π_4	-	-	2,700	(1)
π_5	-	-	2,700	(1)
π_d	-	2,700	-	(1)
γ_1	900	900	900	(1)
γ_2	900	900	1320	(1,6)
γ_3	-	900	900	(1)
X	500	500	500	(1)
Y	1,000	1,000	1,000	(1)
n_1	40	40	40	(7)
n_2	70	70	70	(7)
n_3	-	4	4	(7)
K_{p1}	-	1.8×10^4	-	(3)
K_{p2}	-	-	1.8×10^4	(3)
K_{IS}	-	-	1700	(6)
K_{AD}	-	100	-	(3)
K_{u1}	5	5	5	(1)
K_{u2}	-	5	5	(1)
[3OC6] (u_1)	0 - 1,000	0 - 1,000	0 - 1,000	this study [b]
[aTc] (u_2)	-	108	108	this study [b]

[a] k is the dissociation constant of a ribosome binding to the corresponding ribosome binding site, in nM; κ is the dissociation constant of a promoter binding to RNA polymerase, in nM; δ is the mRNA decay rate, in h^{-1}; λ is the protein decay rate, in h^{-1}; π is the protein production rate, in h^{-1}; γ is the transcription rate, in h^{-1}; X is the total concentration of RNA polymerase, in nM; Y is the total concentration of ribosome, in nM; n is the plasmid concentration, in nM; the units of K are: nM (K_p), nM^2 (K_u), nM (K_{AD}), and nM^2 (K_{IS}); and u is the inducer concentration, in nM. Subscript '*1*' represents RFP, '*2*' represents GFP, '*3*' represents ExsA, '*4*' represents InvF, and '*5*' represents SicA. The subscript '*d*' represents the protein in the negative feedback loop.

[b] Those parameter values were based on the experimental values or estimated values in this study.

[c] k_2 was 1.4×10^6 and 4.6×10^5 for *gfp* with different RBSs in Figure 5B and 5C, respectively.

[d] For Figure 5C, k_d was 2×10^4 due to the modified RBS.

[e] κ_1 values of 0.05 - 10,000 nM were used for Figure 3. For Figure 5, κ_1 was 2,500 nM.

Table S3. Parameters of pLux* promoter transfer functions. The transfer functions were obtained by fitting the experimental data to the Hill equation: $F = F_{min} + (F_{max} - F_{min}) \frac{L^{\eta}}{K_D^{\eta} + L^{\eta}}$, where L is the concentration of 3OC6, F is the pLux* promoter activity, F_{min} is the basal activity due to promoter leakiness, F_{max} is the maximum activity, η is the Hill coefficient, and K_D denotes the input threshold where the output is half-maximal. The ± values represent the 95% confidence interval. Nucleotides highlighted in red (also in upper case) denote point mutations introduced in the original pLux* promoter sequence. Underlined sequences denote the -35 and -10 regions of the pLux* promoter.

Promoter	DNA Sequence (5' – 3')	η	K_D (nM)	F_{min} x 10^2 (REU)	F_{max} (REU)	R^2
Original	caggtttacgcaagaaaatggtttgttactttcgaa	1.92 ± 0.11	4.03 ± 0.15	1.49 ± 0.22	3.96 ± 0.03	0.9996
-10N1A	caggtttacgcaagaaaatggtttgtAactttcgaa	1.59 ± 0.09	6.85 ± 0.59	4.04 ± 0.26	2.37 ± 0.07	0.9988
-10N2T	caggtttacgcaagaaaatggtttgttTctttcgaa	1.73 ± 0.03	5.75 ± 0.20	6.51 ± 0.31	6.88 ± 0.21	0.9995
-10N3A	caggtttacgcaagaaaatggtttgttaAtttcgaa	1.80 ± 0.07	3.11 ± 0.19	6.78 ± 0.59	13.90 ± 0.33	0.9974
-10N4A	caggtttacgcaagaaaatggtttgttacAttcgaa	2.40 ± 0.63	1.14 ± 0.32	16.57 ± 2.25	11.22 ± 0.50	0.9874
-35N1A	caggAttacgcaagaaaatggtttgttactttcgaa	1.62 ± 0.06	8.99 ± 0.47	3.43 ± 0.13	3.58 ± 0.02	0.9997
-35N1G	caggGttacgcaagaaaatggtttgttactttcgaa	1.64 ± 0.01	9.84 ± 0.93	3.57 ± 0.14	6.77 ± 0.19	0.9986
-35N3A	caggttAacgcaagaaaatggtttgttactttcgaa	1.54 ± 0.06	8.61 ± 0.47	3.65 ± 0.20	9.34 ± 0.15	0.9986
-35N4G	caggtttGcgcaagaaaatggtttgttactttcgaa	1.71 ± 0.10	7.15 ± 0.59	3.83 ± 0.24	9.76 ± 0.18	0.9979
-35N5T	caggtttaTgcaagaaaatggtttgttactttcgaa	1.74 ± 0.08	7.81 ± 0.74	5.94 ± 0.16	8.72 ± 0.55	0.9874
-35N5G	caggtttaGgcaagaaaatggtttgttactttcgaa	1.44 ± 0.06	9.83 ± 1.64	3.78 ± 0.24	5.59 ± 0.52	0.9996

Table S4. Plasmids used in this study.

Plasmid Name	Origin	Resistance	Properties
pTS410	p15A	SpecR	pLux-*rfp*_-10N1A
pTS411	p15A	SpecR	pLux-*rfp*_-10N2T
pTS412	p15A	SpecR	pLux-*rfp*_-10N3A
pTS413	p15A	SpecR	pLux-*rfp*_-10N4A
pTS414	p15A	SpecR	pLux-*rfp*_-35N1A
pTS415	p15A	SpecR	pLux-*rfp*_-35N1G
pTS416	p15A	SpecR	pLux-*rfp*_-35N3A

pTS417	p15A	SpecR	pLux-*rfp*_-35N4G
pTS418	p15A	SpecR	pLux-*rfp*_-35N5T
pTS419	p15A	SpecR	pLux-*rfp*_-35N5G
pTS217	p15A	SpecR	pLux-*rfp*_Original
pTS354	pSC101*	AmpR	pLux-*rfp*_-35N4G
pTS224	p15A	SpecR	pcI-*gfp*
pTS443	ColE1	CmR	pcI-*gfp*
pTS005	ColE1	CmR	pexsD-*gfp*
pTS617	ColE1	CmR	pexsD-(AGGAGT→GATTAT)-*gfp*
pTS618	ColE1	CmR	pexsD-(AGGAGT→TTTGCT)-*gfp*
pTS227	pSC101*	KanR	pTet*-*exsA*
pTM008	ColE1	CmR	psicA-*gfp*
pTS226	pSC101*	AmpR	pTet*-*invF-sicA*
pTS493	ColE1	CmR	pexsD-*gfp-exsD*
pTS616	ColE1	CmR	pexsD-*gfp*-(TGAGGA→CGATAA)-*exsD*
pTS612	ColE1	CmR	pexsD-*gfp-exsD***
pTS657	ColE1	CmR	pexsD-(AGGAGT→CAGGGT)-*gfp_4-exsD***
pTS658	ColE1	CmR	pexsD-(AGGAGT→GTAAGT)-*gfp_6-exsD***
pTS660	ColE1	CmR	pexsD-(AGGAGT→ATTGTT)-*gfp_8-exsD***
pAH016	ColE1	CmR	BBa-J23104-*gfp*
pAH034	p15A	KanR	BBa-J23105-*rfp*

Table S5. Strains used in this study.

Name	Host Strain	Plasmids	Figure
TS368	DH10B	pTS354 + pTS224	Fig. S1
TS464	DH10B	pTS354 + pTS443	Fig. S1
TS451	DH10B	pTS417 + pTS443	Fig. S1
TS451	DH10B	pTS417 + pTS443	Fig. 2, Fig. S2
TS427	DH10B	pTS417 + pTS227 + pTS005	Fig. 2, Fig. S2
TS440	DH10B	pTS417 + pTS226 + pTM008	Fig. 2, Fig. S2
TS410	DH10B	pTS410	Fig. S3
TS411	DH10B	pTS411	Fig. S3
TS412	DH10B	pTS412	Fig. S3
TS413	DH10B	pTS413	Fig. S3
TS414	DH10B	pTS414	Fig. S3
TS415	DH10B	pTS415	Fig. S3

TS416	DH10B	pTS416	Fig. S3
TS417	DH10B	pTS417	Fig. S3
TS418	DH10B	pTS418	Fig. S3
TS419	DH10B	pTS419	Fig. S3
TS217	DH10B	pTS217	Fig. S3
TS444	DH10B	pTS410 + pTS443	Fig.3, Fig. S3
TS445	DH10B	pTS411 + pTS443	Fig.3, Fig. S3/S5
TS446	DH10B	pTS412 + pTS443	Fig.3, Fig. S3
TS447	DH10B	pTS413 + pTS443	Fig.3, Fig. S3/S5
TS448	DH10B	pTS414 + pTS443	Fig.3, Fig. S3
TS449	DH10B	pTS415 + pTS443	Fig.3, Fig. S3
TS450	DH10B	pTS416 + pTS443	Fig.3, Fig. S3
TS451	DH10B	pTS417 + pTS443	Fig.3, Fig. S3
TS452	DH10B	pTS418 + pTS443	Fig.3, Fig. S3
TS453	DH10B	pTS419 + pTS443	Fig.3, Fig. S3
TS454	DH10B	pTS217 + pTS443	Fig.3, Fig. S3
TS420	DH10B	pTS410 + pTS227 + pTS005	Fig.3, Fig. S3
TS421	DH10B	pTS411 + pTS227 + pTS005	Fig.3, Fig. S3
TS422	DH10B	pTS412 + pTS227 + pTS005	Fig.3, Fig. S3
TS423	DH10B	pTS413 + pTS227 + pTS005	Fig.3, Fig. S3
TS424	DH10B	pTS414 + pTS227 + pTS005	Fig.3, Fig. S3
TS425	DH10B	pTS415 + pTS227 + pTS005	Fig.3, Fig. S3
TS426	DH10B	pTS416 + pTS227 + pTS005	Fig.3, Fig. S3
TS427	DH10B	pTS417 + pTS227 + pTS005	Fig.3, Fig. S3
TS428	DH10B	pTS418 + pTS227 + pTS005	Fig.3, Fig. S3
TS429	DH10B	pTS419 + pTS227 + pTS005	Fig.3, Fig. S3
TS430	DH10B	pTS217 + pTS227 + pTS005	Fig.3, Fig. S3
TS433	DH10B	pTS410 + pTS226 + pTM008	Fig.3, Fig. S3
TS434	DH10B	pTS411 + pTS226 + pTM008	Fig.3, Fig. S3
TS435	DH10B	pTS412 + pTS226 + pTM008	Fig.3, Fig. S3
TS436	DH10B	pTS413 + pTS226 + pTM008	Fig.3, Fig. S3
TS437	DH10B	pTS414 + pTS226 + pTM008	Fig.3, Fig. S3
TS438	DH10B	pTS415 + pTS226 + pTM008	Fig.3, Fig. S3
TS439	DH10B	pTS416 + pTS226 + pTM008	Fig.3, Fig. S3
TS440	DH10B	pTS417 + pTS226 + pTM008	Fig.3, Fig. S3
TS441	DH10B	pTS418 + pTS226 + pTM008	Fig.3, Fig. S3
TS442	DH10B	pTS419 + pTS226 + pTM008	Fig.3, Fig. S3
TS231	DH10B	pTS217 + pTS226 + pTM008	Fig.3, Fig. S3
TS421	DH10B	pTS411 + pTS227 + pTS005	Fig. 5A, Fig. S6A/S7A
TS507	DH10B	pTS411 + pTS227 + pTS493	Fig. 5A/5B, Fig. S6A/S6B/S7B/S8B

TS623	DH10B	pTS411 + pTS227 + pTS618	Fig. 5B, Fig. S6B/S8A
TS621	DH10B	pTS616 + pTS227 + pTS217	Fig. 5C, Fig. S6C
TS622	DH10B	pTS617 + pTS227 + pTS217	Fig. 5C, Fig. S6C
TS613	DH10B	pTS411 + pTS227 + pTS612	Fig. S7C
TS651	DH10B	pTS411 + pTS227 + pTS657	Fig. S8C
TS652	DH10B	pTS411 + pTS227 + pTS658	Fig. S8D
TS654	DH10B	pTS411 + pTS227 + pTS660	Fig. S8E
AH016	DH10B	pAH016	Entire paper
AH034	DH10B	pAH034	Entire paper

Table S6. Genetic parts used in this study.

Part Name	Type and Source	DNA sequence
exsA	Gene (8)	atgcaaggagccaaatctcttggccgaaagcagataacgtcttgtcattggaacattccaactttcgaatacagggtaaacaaggaa gagggcgtatatgttctgctcgagggcgaactgaccgtccaggacatcgattccacttttgcctggcgcctggcgagttgcttttcgt ccgccgcggaagctatgtcgtaagtaccaagggaaaggacagccgaatactctggattccattatctgcccagtttctacaaggctt cgtccagcgcttcggcgcgctgttgagtgaagtcgagcgttgcgacgagcccgtgccgggcatcatcgcgttcgctgccacgcct ctgctggccggttgcgtcaaggggttgaaggaattgcttgtgcatgagcatccgccgatgctcgcctgcctgaagatcgaggagtt gctgatgctcttcgcgttcagtccgcaggggccgctgctgatgtcggtcctgcggcaactgagcaaccggcatgtcgagcgtctgc agctattcatggagaagcactacctcaacgagtggaagctgtccgacttctcccgcgagttcggcatggggctgaccaccttcaag gagctgttcggcagtgtctatggggtttcgccgcgcgcctggatcagcgagcggagaatcctctatgcccatcagttgctgctcaac agcgacatgagcatcgtcgacatcgccatggaggcgggcttttcagtcagtcctatttcacccagagctatcgccgccgtttcggc tgcacgccgagccgctcgcggcaggggaaggacgaatgccgggctaaaaataactga
exsD	Gene (8)	atggagcaggaagacgataagcagtactcccgagaagcggtgttcgctggcaggcgggtatccgtggtgggctcggacgcccg ctcgcggggtcgggtgccgggttacgcatcgagcagtttgtatcgtgagtccggaatcatcagtgcgcggcaactggcgttgctgc agcggatgctgccgcgcctgcggctggagcaactgttccgctgcgagtggttgcagcagcgcctggcgcgcggcctggcgctg gggcgcgaagaggtgcggcagattctcctctgcgcggcgcaggacgacgacggctggtgctccgaactgggcgaccgggtca acctcgccgtgccgcagtcgatgatcgactgggtcctgctgccggtctatggctggtgggaaagcctgctcgaccaggcgatccc cggctggcgcctgtcgctggtggagctggagacccagtcccggcaactgcgagtcaagtccgaattctggtcccgcgtggccga gctggagccggagcaggcccgcgaggaactggccagggtcgccaagtgccaggcgcgcacccaggaacaggtggccgaact ggccggcaagctggagacggcttcggcactggcgaagagcgcctggccgaactggcagcggggcatggcgacgctgctcgcc agcggcgggctggccggcttcgagccgatccccgaggtcctcgaatgcctctggcaacctctctgccggctggacgacgacgtc ggcgcggcggacgccgtccaggcctggctgcacgaacgcaacctgtgccaggcacaggatcacttctactggcagagctga
invF	Gene (2)	atgctaaatacgcaggaagtacttaaagaaggagagaagcggaaaatccgcagcccggaagcatggtttatacagacgtgttccg cgcaaaagctgcatatgtcattttctgaaagccgacacaatgaaaattgcctgattcaggaaggcgcgctgctttttgcgagcaggc cgttgtcgcaccagtatcaggagacctggtttttcgaccgttaaaaattgaagtactcagcaaattactggcatttatcgatggcgcag gattagtggacacgacatatgctgaatccgataaatgggttttgctgagtcctgagtttcgcgctatttggcaagatcgtaaacgctgc gagtactggttttgcagcaaattattacgccttctccggccttcaataaggtactggcgctgttacgaaaaagcgagagttactggttg gttggctatttactcgctcagtcaaccagcggcaacacgatgagaatgctgggagaagactatggcgtttcttataccatttcgtcg tttgtgcagcagagcgttgggcggaaaagcgaagagtgaattacgaaactggcgtatggcgcaatcgctgctgaatagtgtagaa ggccacgagaacatcacccaattagccgttaatcatggttactcatcgccttcacatttttctagtgagatcaaagagctgatcggcgtt tcgccgcggaaattatcaaatattattcaattggcagacaaatga
*sicA**	Gene (2)	atggattatcaaaataatgtcagcgaagaacgtgttgcggaaatgatttgggatgccgttagtgaaggcgccacgctaaaagacgtt catgggatccctcaagatatgatggacggtttatatgctcatgcttatgagttttataaccagggacgactggatgaagctgagacgtt ctttcgttacttatgcatttatgatttttacaatcccgattacaccatgggactggcggcagtatgccaactgaaaaaacaatttcagaaa gcatgtgacctttatgcagtagcgtttacgttacttaaaaatgattatcgccccgttttttttaccgggcagtgtcaattattaatgcgtaag gcagcaaaagccagacagtgttttgaacttgtcaatgaacgtactgaagatgagtctctgcgggcaaaagcgttggtctatctggag gcgctaaaaacggcggagacagagcagcacagtgaacaagaaaaggaataa

gfp	Gene (6)	atgagtaaaggagaagaacttttcactggagttgtcccaattcttgttgaattagatggtgatgttaatgggcacaaattttctgtcagtg gagagggtgaaggtgatgcaacatacggaaaacttacccttaaatttatttgcactactggaaaactacctgttccatggccaacactt gtcactactttgacttatggtgttcaatgcttttcaagatacccagatcatatgaaacggcatgactttttcaagagtgccatgcccgaag gttatgtacaggaaagaactatatttttcaaagatgacgggaactataagacacgtgctgaagtcaagtttgaaggtgatacacttgtta atagaatcgagttaaaaggtattgattttaaagaagatggaaacattcttggacacaagttggaatacaactataactcacacaatgtat acatcatggcagacaaacaaaagaatggaatcaaagttaacttcaaaattagacacaacattgaagatggaagcgttcaactagca gaccattatcaacaaaatactccaattggcgatggccctgtccttttaccagacaaccattacctgtccacacaatctgccctttcgaaa gatcccaacgaaaagagagaccacatggtccttcttgagtttgtaacagctgctgggattacacatggcatggatgaactatacaaa aggcctgcagcaaacgacgaaaactacgcttaa
rfp	Gene (9)	atggcgagtagcgaagacgttatcaaagagttcatgcgtttcaaagttcgtatggaaggttccgttaacggtcacgagttcgaaatcg aaggtgaaggtgaaggtcgtccgtacgaaggtacccagaccgctaaactgaaagttaccaaaggtggtccgctgccgttcgcttg ggacatcctgtccccgcagttccagtacggttccaaagcttacgttaaacacccggctgacatcccggactacctgaaactgtccttc ccggaaggtttcaaatgggaacgtgttatgaacttcgaagacggtggtgttgttaccgttacccaggactcctccctgcaagacggt gagttcatctacaaagttaaactgcgtggtaccaacttcccgtccgacggtccggttatgcagaaaaaaaccatgggttgggaagctt ccaccgaacgtatgtacccggaagacggtgctctgaaaggtgaaatcaaaatgcgtctgaaactgaaagacggtggtcactacga cgctgaagttaaaaccacctacatggctaaaaaaccggttcagctgccgggtgcttacaaaaccgacatcaaactggacatcacct cccacaacgaagactacaccatcgttgaacagtacgaacgtgctgaaggtcgtcactccaccggtgcttaa
pexsD	Promoter (8)	gaaggacgaatgccgggctaaaaataactgacgtttttgaaagcccggtagcggctgcatgagtagaatcggcccaaat
psicA	Promoter (6)	ccacaagaaacgaggtacggcattgagccgcgtaaggcagtagcgatgtattcattgggcgtttttg
pcI	Promoter	tttctggaattctctagatttgacatacctctggcggtgatatataatggttgcaag
pTet*	Promoter (2)	ttttcagcaggacgcactgacctccctatcagtgatagagattgacatccctatcagtgatagagatactgagcacatat
pLux*_-10N1A	Promoter	acctgtaggatcgtacaggtttacgcaagaaaatggtttgt**A**actttcgaataaa
pLux*_-10N2T	Promoter	acctgtaggatcgtacaggtttacgcaagaaaatggtttgtt**T**ctttcgaataaa
pLux*_-10N3A	Promoter	acctgtaggatcgtacaggtttacgcaagaaaatggtttgtta**A**tttcgaataaa
pLux*_-10N4A	Promoter	acctgtaggatcgtacaggtttacgcaagaaaatggtttgttac**A**ttcgaataaa
pLux*_-35N1A	Promoter	acctgtaggatcgtacagg**A**ttacgcaagaaaatggtttgttactttcgaataaa
pLux*_-35N1G	Promoter	acctgtaggatcgtacagg**G**ttacgcaagaaaatggtttgttactttcgaataaa
pLux*_-35N3A	Promoter	acctgtaggatcgtacaggtt**A**acgcaagaaaatggtttgttactttcgaataaa
pLux*_-35N4G	Promoter	acctgtaggatcgtacaggttt**G**cgcaagaaaatggtttgttactttcgaataaa
pLux*_-35N5T	Promoter	acctgtaggatcgtacaggttta**T**gcaagaaaatggtttgttactttcgaataaa
pLux*_-35N5G	Promoter	acctgtaggatcgtacaggttta**G**gcaagaaaatggtttgttactttcgaataaa
pLux*_Original	Promoter (2)	acctgtaggatcgtacaggtttacgcaagaaaatggtttgttactttcgaataaa
BBa_J23104	Promoter (http://parts.igem.org/Promoters/Catalog/Anderson)	ttgacagctagctcagtcctaggtattgtgctagc
BBa_J23105	Promoter (http://parts.igem.org/Promoters/Catalog/Anderson)	tttacggctagctcagtcctaggtactatgctagc

References

1. Gyorgy, A., Jiménez, J.I., Yazbek, J., Huang, H.-H., Chung, H., Weiss, R. and Del Vecchio, D. (2015) Isocost lines describe the cellular economy of genetic circuits. *Biophys. J.*, **109**, 639-646.
2. Moon, T.S., Lou, C.B., Tamsir, A., Stanton, B.C. and Voigt, C.A. (2012) Genetic programs constructed from layered logic gates in single cells. *Nature*, **491**, 249-253.
3. Shopera, T., Henson, W.R., Ng, A., Lee, Y.J., Ng, K. and Moon, T.S. (2015) Robust, tunable genetic memory from protein sequestration combined with positive feedback. *Nucleic acids research*, **43**, 9086-9094.
4. Rosenfeld, N., Young, J.W., Alon, U., Swain, P.S. and Elowitz, M.B. (2005) Gene regulation at the single-cell level. *Science* **307**, 1962-1965.
5. Lykken, G.L., Chen, G., Brutinel, E.D., Chen, L. and Yahr, T.L. (2006) Characterization of ExsC and ExsD self-association and heterocomplex formation. *Journal of bacteriology*, **188**, 6832-6840.
6. Temme, K., Salis, H., Tullman-Ercek, D., Levskaya, A., Hong, S.H. and Voigt, C.A. (2008) Induction and relaxation dynamics of the regulatory network controlling the type III secretion system encoded within Salmonella Pathogenicity Island 1. *J. Mol. Biol.*, **377**, 47-61.
7. Lutz, R. and Bujard, H. (1997) Independent and tight regulation of transcriptional units in Escherichia coli via the LacR/O, the TetR/O and AraC/I1-I2 regulatory elements. *Nucleic Acids Res.*, **25**, 1203-1210.
8. Stover, C.K., Pham, X.Q., Erwin, A.L., Mizoguchi, S.D., Warrener, P., Hickey, M.J., Brinkman, F.S.L., Hufnagle, W.O., Kowalik, D.J., Lagrou, M. *et al.* (2000) Complete genome sequence of Pseudomonas aeruginosa PAO1, an opportunistic pathogen. *Nature*, **406**, 959-964.
9. Salis, H.M., Mirsky, E.A. and Voigt, C.A. (2009) Automated design of synthetic ribosome binding sites to control protein expression. *Nat. Biotechnol.*, **27**, 946-U112.